The Hebrew University of Jerusalem

The Faculty of Mathematics and Sciences

Department of Applied Physics

Increased superconducting properties of Nb thin film, proximity coupled to gold nano particles using linking organic molecules

Eran Katzir

Under the Supervision of: Dr. Yossi Paltiel

Thesis submitted for the degree Master of Science

November 2011

To Yulia

Acknowledgment

I want to thank many people who supported me throughout my entire project.

First, I would like to thank Yossi Paltiel for his guidance and support during the project and the opportunity to work independently while knowing that his door is always open.

Second, I would like to thank Shira Yochelis for her imminent knowledge and the resilience to listen to my whinings.

I would like to thank my friends in the lab for the support and for the great atmosphere that makes the lab a great place to be in. I would like to thank Gregory Litus and Yuri Myasodeyov from Weizmann instituted for the support in measuring the samples. This research could not have been possible without the samples provided by Nadav Katz and Felix Zeides. The STM measurements were performed by Yoav Kalcheim and Oded Millo, I want to thank them also for the help.

Abstract

Charge transfer through organic molecules is hard to monitor and control. In this research we present a novel technique which is sensitive to charge transfer from gold nano dots to superconductor films through a given organic molecules.

The large sensitivity of the measurements originates from the proximity effect which alters the critical current of the Nb film. The change in current is explained by Andreev reflection, meaning charge transfer between the nano-particles and the superconductor through the organic monolayer. The Andreev reflection cause a local superconductor to normal transition, which acts as pinning site for the type II superconductor vortices. The addition of pinning sites translates to critical current enhancement which we were able to observe.

The critical temperature, T_C, of thin Nb films was changed upon the attachment of gold nano-particles through organic linker molecules. Much to our surprise we noticed that the T_C is routinely enhanced with ~3 nm long linker molecules, while with the shorter linkers, a reduction of T_C was observed, possibly due to the "classic" *proximity effect*. The enhancement of the longer linkers or the *inverse proximity effect*, was the strongest for an optimal length of linkers showing an enhancement of the superconductor's T_C by up to ~10% compared to the bare 50nm film.

This effect may be accounted as a new pairing mechanism involving a coupling between electrons at the gold nano-particles and the Nb film, mediated by the vibrations of the organic linker molecules.

VI

Contents

Chapter 1

Introduction and Background

The *proximity effect* (PE) in superconductivity occurs when a superconductor (S) is placed in contact with a normal metal (N). The resulting critical temperature of the superconductor, T_c, is then suppressed and signs of weak superconductivity are induced in N. The *proximity effect* is well understood for 'conventional' BCS superconductors, and is known to take place through Andreev reflections. A hole impinging on the S-N interface from the normal side is retro-reflected as an electron, thus destroying a Cooper-pair in the superconductor. By this, superconductivity is weakened in the superconductor and superconducting correlations are induced in the normal side up to a distance where the electron and the hole lose phase-coherence. Hence, the *proximity effect* requires good electrical contact.

This phenomenon offers a powerful tool to examine the changes in properties of the superconductor and the metal sides of the junction. Moreover, the *Proximity Effect* can probe quantum interfaces effects and the physical mechanism of superconductivity. Even more intriguing, and less common, is the *inverse proximity effects*, where the critical temperature T_c of a superconductor is increased upon attachment to a non-superconducting material.

In our system, while using gold nano particles (NP's) attached by organic monolayer of an appropriate length to the Nb superconductor's surface we have found a strong *inverse proximity effect*, where the critical temperature of the Nb film can be significantly increased. The observed effect strongly depends on the NPs' size, the length of the organic linkers and the Nb film thickness. Recent electron tunneling spectroscopy using STM showed that such an effect modify the gold NPs electronic density of states. This effect may be accounted for by a new pairing mechanism involving a coupling between electrons at the gold nano-particles and the Nb film, mediated by the vibrations of the organic linker molecule. These results may open a way to developed planer lithography and new routes for room-temperature superconducting-normal junction

devices. Achieving this would open up a way to understanding high temperature superconductors mechanisms and exploit them in day a to day devices.

1.1 Superconductivity.

1.1.1 General properties.

Superconductivity was discovered in 1911 by Kamerlingh-Onnes[1] when he found that bellow a well-defined temperature T_c the electrical resistance of some pure metals is zero. Since the conductance become infinite these materials were called superconductors. The zero resistivity characteristic of superconductivity is most appealing from the technological point of view. When the resistance is zero there is no dissipation and thus persistent currents can be obtained. However, if the density of the current flowing through the superconductor is higher than a critical current density J_c there is a finite dissipation. Hence, for technological applications, J_c should be kept as high as possible.

Another important characteristic of superconductors was discovered in 1933 by Meissner and Ochsenfeld and is known as the Meissner effect.[2] Bellow a certain applied critical magnetic field H_c superconductors are perfect diamagnets. The Meissner effect described in 1935 by F. and H. London, predicted that the external magnetic field would decay exponentially at the superconductor surface. The theory predicted a characteristically length scale, λ, London penetration depth, in which the external magnetic field would suppress.[3]

The first microscopic theory that described superconductivity was published in 1957 by Bardeen, Cooper and Schrieffer (BCS).[4] It described the superconductivity as an effect caused by condensation of electrons "Cooper pairs" to a boson like state. Until 1986, it was believed, according to the BCS theory that, superconductivity does not exist at temperatures above 30K, and which explains the origin of all superconductors.

The discovery of the high-temperature superconductors (HTSC) in 1986 renewed the interest in the research of superconductivity.[5] The characteristics of the new materials are interesting both from the technological and the scientific point of view. The great advantage of having a superconductor material above liquid nitrogen temperature is obvious. Indeed, many technological applications such as high field magnets, energy storage devices etc. may use HTSC. The main technologic drawbacks of HTSC are the relatively low critical currents, and the difficulties in manufacturing wires and cables from these materials. An immense development effort is directed to solving these two problems.

1.1.2 BCS theory

In 1957, Bardeen, Cooper and Schrieffer published the "Macroscopic theory of superconductivity", [4] later known as the BCS theory (received the Nobel price at 1972). For the first time, the theory explained the superconductivity as a condensation of electrons to a boson like state. The basic idea of the theory considered a pair of electrons (Cooper pair) that interact with each other due to the material phonon attraction and therefore screen the coulomb repulsion.[6] Even if the attraction is weak and the bounding energy is small, it can still be enough to form the superconducting state. In more details, the bound state occurs due to electron polarization of the surrounding medium by attracting the positive ions. In turn, the ions attract the second electron, forming a net of attractions between the electrons. If the attraction is strong enough to overcome the electrons coulomb repulsion, and the phonon energy is small enough (below the critical temperature), a superconducting state with Copper pair is formed.

In zero temperature there are no phonons in the system. If an electron with a momentum k_1 is moving in the matter, a phonon with momentum q is formed. When a second electron interact with the phonon, it changes his momentum to $k_{2'}$. From the momentum conservation we can see that $k_1+k_2=k_1+k_{2'}$ and the phonon momentum is $q=k_1-k_{1'}$. The local change in the electron density due to the creation of the phonon q causes a local oscillations in the electron density with a frequency of $\omega_e = \left(\varepsilon_{k1} - \varepsilon_{k1'}\right)/\hbar$

when ε_{k1} and $\varepsilon_{k1'}$ are the electron energy and k$_1$ and k$_{1'}$ are the momentums respectively. A change in the local electron density will cause the ions in the lattice to balance the change by attracting to it. Due to the great ions mass, oscillations will occur in the Debye characteristic frequency ω_D, the maximum of lattice vibrations. In turn, a second electron will be attracted due to the change in the positive ion density. Since the attraction between the electrons is mediated by their interaction with the phonons, the interaction frequency $\omega_c = \omega_D$. Consequently, the role of the temperature in the BCS theory is called Debye temperature $\Theta_D = \hbar\omega_D/k$. According to the BCS theory, in superconductors the Debye temperature is predicted to be less then 25 Kelvin degrees and therefore the phonon mechanism cannot lead to high temperature superconductors.

The BCS theory maintained as the main theory of superconductivity until the discovery of high Tc superconductors in 1986. Those required a new model to understand the second type of superconductors.

1.1.3 Type II superconductors

Superconductors are usually divided into two types according to the manner they break under magnetic field. Type I superconductors break down when the magnetic field applied raises above a critical value H_c. In type II superconductors when the magnetic field raises above the critical value H_{c1}, a mixed state or vortex state is created which results in a second critical value of H_{c2} that breaks the superconductivity.

The origin of type II superconductivity is discussed in the Ginzburg-Landau (GL) theory[7], named after V.L Ginzburg and L. Landau. The theory defines the coherence length, ζ, as the free path of the charge carriers inside the superconductor. With London penetration depth, λ, GL theory propose a ratio of the two characteristic lengths, $\kappa = \lambda/\zeta$. For classic pure superconductors it was found that $\kappa < 1$. In 1957, A. A. Abrikosov investigated the effect of $\kappa > 1$ on GL theory.[8] Abrikosov entitled his prediction as type II due to dramatically different behavior of the superconductor. He showed that instead of

breaking the superconductivity gradually by applying external magnetic field like in type I; in type II superconductors after a certain critical point, H_{c1}, a magnetic flux penetrates the superconductor as a flux vortices lattice until a second critical point, H_{c2}, where the superconductivity breaks (received Nobel price 2003). The possibility of flux penetration to the superconductor in an ordered flux lattice state reduce the free energy, therefore H_{c2} is larger then H_c. Moreover, Abrikosov showed that the penetration of the magnetic flux lattice is ordered in a triangular array. Each vortex has a "core" containing non-supercurrent with a size of $\sim \zeta$ diameter. However, the supercurrents surrounding the core arrange themselves so that the total magnetic flux through the core is quantized and carries a quantum of flux,

$$(1) \qquad\qquad \phi_0 = \frac{hc}{2e} = 2.07 \times 10^{-7} \ G/cm$$

Where h is Planck's constant, c is the speed of light and e is the elementary charge.

A supercurrent in the superconductor surrounds each flux vortex and contains the current inside the vortex to the center. By applying transport current through the superconductor the vortices experience Lorentz force $J \times \phi_0$ per unit length, where J is the current density. This force makes them move sideways producing a longitudinal voltage that in turn induces resistance. It is known, that in high purred materials the critical current, which force the vortex to move, is much smaller than in low purred materials[9]. However, in inhomogeneous material there are defects that pin the vortex until a higher critical current is reached and the Lorentz force exceeds the pinning force and compels the vortex to move and to induce resistance. This method of pinning the vortices to increase the amount of current inside the superconductor is a leading technique to improve the superconductor's properties and induce superconductor with higher critical current.[10]

High Tc superconductors are type II. Until now many theories proposed to describe their high critical temperature value but none of them succeeded to fully describe their properties.

1.1.4 Ginzburg Prediction

In 2003, the noble committee nominated Vitaly L. Ginzburg to the noble prize award in physics on the GL theory. In his noble prize lecture he refers to a model made by Little in 1964[11], which suggested a new threshold level for superconductors phase transition. Little suggested replacing the phonon mechanism of attraction, proposed by the BCS theory, with electron bound pairing in the system (excitonic mechanism). Bound pairing may vary from other electrons to molecules, dielectric, etc. The theory is based on the existence of oscillation (vibration) modes, for example in the organic molecules which are larger than the oscillations of the electrons in the superconductor proposed by the BCS theory. These oscillations change the electron density in the system by higher frequency proposed by the BSC theory. Hence, the coupling of Cooper pairs is stronger and the critical temperature of the superconductor can be larger. Little calculation showed that in this way his threshold level is larger in two orders of magnitude then the BSC threshold level. His theory, based on layered components of dielectric and metals, contributed to the explanation of high *Tc* superconductivity. As for now, no one ever confirmed Little's theory.

In his nobel lecture, Ginzburg predicted that Little's model can be proven true by realizing artificial dielectric and metal material., *"...the most promising materials- from the point of view of the possibility of raising Tc- are, apparently, layered compounds and dielectric-metal-dielectric sandwiches."* [12]

1.1.5 Proximity Effect and Andreev Reflection

Proximity Effect occurs in the interface between superconductor and a normal metal (N) that found in electrical contact. By having S/N junction there is a diffusion of cooper pairs from the S to the N until the phase coherence is lost far inside the N. This process "weaken" the S properties close to the interface at a length of coherence length, ξ_S, due to a reduction in Cooper pair density, while S properties are induced into the N over a corresponding length,

Normal Metal   Superconductor

ξ_N ξ_S
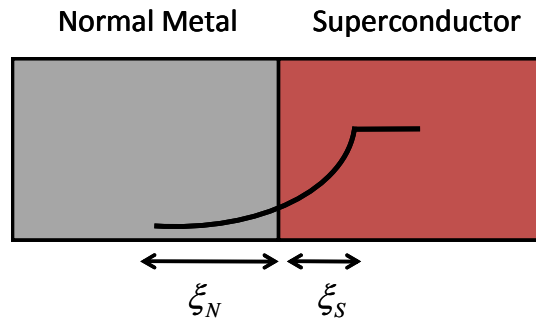
Figure 1: The diffusion of cooper pairs from the superconductor, on a scale of the coherence length, to the normal metal cause superconducting properties to the metal on the account of weakens the superconductor.

ξ_N (see figure 1). The physical notation that governs the effects of S/N junction results from Proximity Effect is referred to as the Andreev Reflection (AR).

In such S/N junction, the Andreev reflection occurs when the propagating electron in N has a smaller energy than the superconductor's energy gap (Δ). Therefore, an electron approaching the junction from the N side cannot propagate, since there are no available states of the same energy in the S side (see figure 2). An incoming electron can be transferred into the S only if a second electron is also transferred through the interface to form a Cooper pair. This process is equivalent to a reflection of a hole.

Since the metal has equal density of states of both spin up and spin down, the propagated electron with spin up reflected back to the N side as a hole with spin down while a Cooper pair is forming in the condensate state of the S. The reflected hole at the interface carries not only an opposite spin to the propagating electron, but also the S phase coherency. By that, the propagating electron and the retro-reflected hole can be coupled to Cooper pair until the phase coherence breaks inside the N. For kT and eV << Δ, all the incident electrons are Andreev reflected.
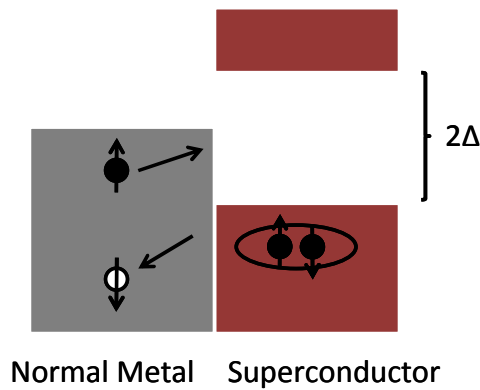
Figure 2: Schematic drawing of energy bands of the S/N junction. The Andreev reflection occurs at the interface by the propagating electron (black) and retro-reflection of a hole(white).

1.1.6 Superconductors Peak Effect

In type II superconductor the critical current can sometimes display an anomaly in the vicinity of the superconductor-metal transition. In this region, the critical current suddenly increases with temperature instead of falling to zero smoothly. This phenomenon is known as the superconductors peak effect (SPE).[13] Usually this phenomenon is ascribed to vortex lattice phase transition, as discussed previously in section 1.1.3.

In the mixed state electrical current exerts a Lorentz force on the vortices, resulting in vortex motion and a resistive electric field. This actually means that if the vortices are free to move there always exist finite resistivity. Fortunately, in any material there are structural defects and inhomogeneities, at which the order parameter is suppressed. The normal core of a vortex is attracted to such defects due to the reduced vortex energy at these locations. The defects pin the vortices preventing them from moving. The minimal threshold current required to overcome the pinning force is the critical current.

At lower temperature the thermal vortex energy is reduced, thus increasing the force required for releasing the vortex from the pinning site. This is why the critical current usually decreases as temperature increases. However, at temperatures close to T_C
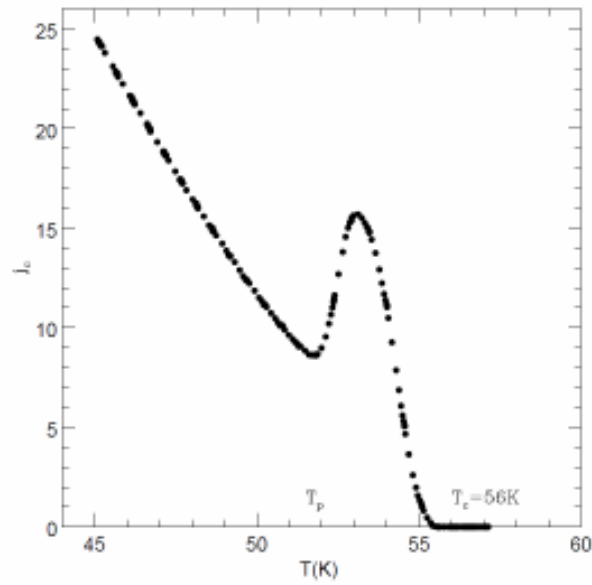
Figure 3: Critical current density of type II superconductor YBCO as a function of temperature. The peak in the current ascribed to the trapping of the vortices by the pinning landscape. This figure extracted from[14].

the anomalous enhancement of the critical current exists. Now it is believed that the peak-effect indicate a structural transformation of the vortex lattice. Bellow the peak region an ordered phase is present, dominated by the elastic energy of the lattice and therefore weakly pinned. Upon approaching the peak effect region, however, the increased softening of the lattice causes a transition into a disordered phase, which better accommodates to the pinning landscape, resulting in the increase of the critical current (see figure 3). Thus, many type-II superconductors display maximum critical current just below $H_{c2}(T)$.[15,16]

Previous studies in niobium single-crystal have revealed an intriguing picture of the peak effect in weakly pinned conventional superconductors. [17] Inducing the peak effect in superconductors can be performed by defects due to ion implantation, or by proximity effect with normal metal.[18]

1.2 Organic Monolayer

1.2.1 Self-Assembled Monolayer

Organic molecules enable nanoscopic molecular architecture and exhibit electrical, magnetic and optical properties for electronic devices while maintaining the flexibility, transparency and ease of assembly. One of the pioneers in organic molecules self assembly was Sagiv in the 80's.[19] He found the possibility of coating a substrate with organic monolayer or multilayer by immersing the substrate in organic solution containing the molecules. This method enables the formation of ordered self assembled layers on top of almost any substrate.

Self-assembled monolayer (SAM) formation may be induced by strong chemisorption between the substrate and the head group of the organic molecule. SAMs coupled to a reading device provide an excellent tool to monitor and probe minor changes that occur at the molecule-substrate interface. These changes can arise from electron tunneling to the surface or from a change in the electron distribution on the surface. The change depends on the chemical bond between the substrate and the molecule head group. By adsorbing different head groups such as thiols, silanes, acids or amines one can modify the surface properties and provide flexible possibilities of dipole direction, hydrophilic or hydrophobic control, chemical sensors etc. [20,21]

It was demonstrated previously, that by adsorbing organic monolayer onto type II superconductor surface the critical current was suppressed[22], and the critical temperature was not changed in these conditions. The suppression of the critical current relates to the capturing of surface defects by the monolayer. Therefore, more vortices stay non-trapped or trapped with lower pinning forces. As described before the non-trapped vortices move perpendicularly to the current and lead to energy dissipation and hence to resistance.

In our work the molecules are used as linkers to control the coupling between nano particles and superconductor wave functions. The possibility of using molecules with different length and conductivity and the possibility to control the head and tail groups, enables to manage the nano structure layer by layer.

1.2.2 The organic monolayer used in my work.

The bonds between the organic molecules and the substrate depend on the substrate type. Therefore, for each substrate a different organic linker is used. It is well known that a native oxide layer is formed on Niobium bulk[23]. In this work, the organic molecule binds to this oxide layer based on silane head group to form the SAM. The silane-oxide bond is well known and found in nature in vast amounts in the form of Silica (silicon dioxide). [24] We used four kinds of molecules silane-based head groups.

Each of the chosen molecules differs in chemical components and length. The molecule contains one or more carbon atoms that are coupled together in covalent bonds. In our work, diversity of bonds between the carbon atoms were used which gives rise to different coupling efficiency due to the difference in the coupling of electronic orbital. More specifically, single carbon-carbon bond, made of sigma bond type, and double carbon-carbon bond, made of pi bond type. The pi bond consists of delocalized electrons and give better conductivity through the molecule[25] compared to sigma bond that has lower electron mobility[26]. Another important parameter in my study was the molecule length that indicates the coupling efficiency. The chosen length of the four SAMs influenced strongly on our results.

The tail group of the organic molecule was chosen to form chemical bond with the gold nano particles. In this case three kinds of tail groups were used; two groups that form covalent bond with the gold nano-particles and one molecule that ends with CH_3 that cannot bind with the gold nano particles. These three kinds of tail groups were specifically chosen to differ in the electronic coupling between the gold nano particles and the superconductor.

The four types of self-assembled monolayer used are the following organic molecules (see figure 4): (a) 3-methylpropane bis-trichlorosilane (diSilane), (b) mercapto propyl silane (MPS), (c) 1,6-Bis(trichlorosilyl)hexane (Hex diSilane) and (d) octadecyl trichlorosilane (OTS) molecules, on which the Au NPs were only physisorbed and thus acted merely as a spacer layer.[22,27,28,29]
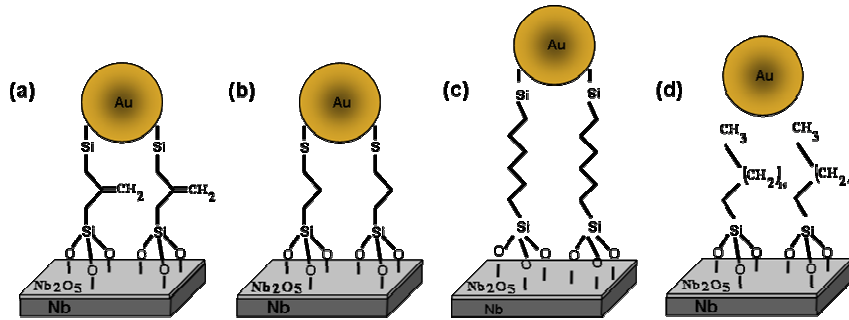
Figure 4: Au NP's attached by self assembled monolayer on top Nb superconductor film. (a) 3-methylpropane bis-trichlorosilane (diSilane), (b) mercapto propyl silane (MPS), (c) 1,6-Bis(trichlorosilyl)hexane (Hex diSilane) and (d) octadecyl trichlorosilane (OTS).

1.3 Nano Particles

1.3.1 General Properties

Nano particles (NPs) approximately 1-100 nm in size, have a significant impact in many scientific fields, including chemistry, material sciences, biology, medicine and electronics. The physical, material and chemical properties of the NPs are directly related to their intrinsic compositions, apparent sizes and surface structures. Within the last few years, advances in micro-fabrication techniques have allowed researches to create unique quantum confinement and thereby opened up a new realm of fundamental physical ideas, as well as the nanostructures devices with dominant quantum mechanical effects[30].

Nanostructure materials derive their special properties from having one or more dimensions that are small compared to the critical length scale of the physical process. For example, in the case of the nanostructure made of metal for electronic transport, the Fermi wavelength or the scattering length is the critical length, which below them the material considered as nanostructure. The confinement of the material to small scales exhibits new observations that could not been seen in large scales before.

In order to understand how size affects material, it is useful to examine the changes that occur at the density of states (DOS), which is how the band structure of the material evolves as a function of the number of atoms in a cluster. This process is illustrated in figure 5, each new pair of interacting atoms produces two new states for
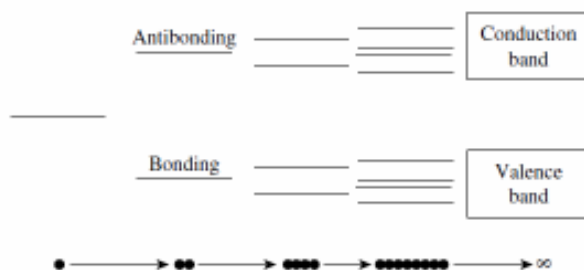
Figure 5: Illustration (extracted from [31]) of the energy levels from one atom to the bulk behavior and the forming of valence and conduction bands.

each atomic state. As more atoms are added to the cluster weaker long range interactions give rise to further small splitting of each of the levels. Eventually, when the cluster size is very large, these two sets of split states become the valence and conduction bands. The largest of DOS occurs at the center of each band. The quantum dots are zero dimensional electronic structure. It confined in three dimensions and therefore the energy is concentrated into discrete levels and the DOS of the structure is series of δ-function peaks[32].

1.3.2 Au Nano Particles Properties

Gold nanoparticles (Au NPs) are one of the elements of core materials available. These particles can be coupled with tunable surface properties in the form of inorganic or inorganic-organic hybrid. Au NPs have been reported as an excellent platform for a broad range of analytical methods.

In any application of Au NPs, it is of particular importance to determine their physical and chemical properties. The scaling down of gold from condensed matter to nanoscale particles produces materials that demonstrate versatile properties. Some of the properties include, long term stability, easy synthesis, shifted emission and illumination at quantum size, melting point reduction, electrical Coulomb blockade effect, surface-to-volume ratio effects, favorable chemical modification, high electro catalytic activity and functional compatibility with molecules. Moreover, organic molecules containing thiols, amino or silane groups can be adsorbed onto gold surface to generate well organized self

assembled monolayers. Molecular assemblies are formed spontaneously by the immersion of the NPs in the molecule solution. Surface modification with functional groups by chemisorptions is the key to prevent the NPs from aggregation and to control the particles size.

The fabrication of structures by means of self assemble has attracted much attention because of the simplicity and flexibility of this approach. The modification of the surface with appropriate chemical bonds can improve the analytical selectivity and to assemble inorganic-organic materials for the purpose of characterization and applications.

Chapter 2

2. The experimental system and method

2.1 CryoFree Spectromag cooler

The system that was used in my experiments is an Oxford's Beta site system. The CryoFree spectromag is a close loop Helium (He_4) cryostat; therefore no liquid Helium is required to be filled in the system. The spectromag can reach 1.5K and 6 to 7 Tesla of magnetic field. The magnetic field lines can be parallel or perpendicular to the sample orientation and can perform in persistence mode. The spectromag is divided to four important sections, the Pulse tube (PT), the superconductor magnet, the Joule Thomson (JT) and the sample space.

The Pulse Tube is the cooling engine of the spectromag; it is the part that governs the system's temperature cool down to 3.5K. The operation of PT is basically thermodynamics and its major advantage is in its fixed parts. The PT components divided
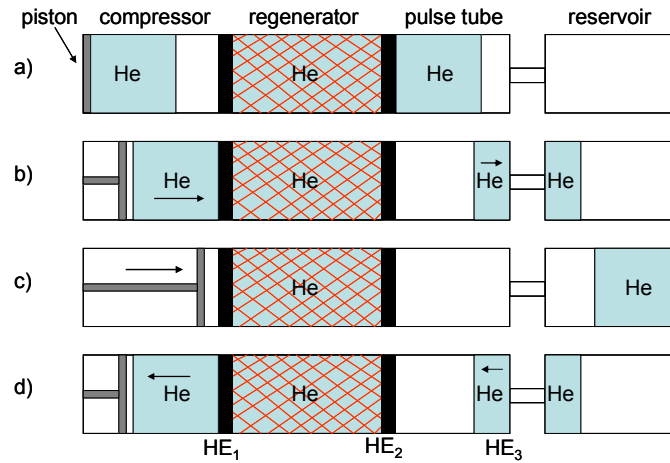
Figure 6: Schematic drawing of the PT cooler cycle containing the compressor, regenerator and pulse tube rooms. The He inside the pulse tube exchange heat with X_2 (a). The piston moves periodicity and pushes the He inside the compressor to exchange heat in X_1 and He gas inside the pulse tube exchange heat in X_3 (b). The He inside the pulse tube and the regenerator are never cross (c and d).

to three parts isolated from room temperature by vacuum (see figure 6). In the PT the external compressor compress the He gas inside the system periodically to the regenerator chamber. The regenerator chamber is containing a porous material and the He movement inside makes the pressure oscillate. As the gas enters the regenerator chamber, it exchanges heat with the porous material. When the He gas is compressed, it is with higher pressure then the reservoir. Consequently, the He in the PT flows to the reservoir through an orifice and exchange heat with the ambient through the heat exchanger, HE_3 at the warm end of the pulse tube chamber. The flow stops when the pressure in the PT and reservoir are equalized. Now the piston moves back and expends the gas adiabatically in the PT. Next, the cold, low pressured gas in the PT is forced to the cold end of the PT, by the gas flow from the reservoir. As the cold gas flows from the heat exchanger at the cold end of the PT it picks up heat from HE_2. The flows continue until the pressure is equalized. Then the cycle repeats. Figure 7 represents the gas elements near HE_3, which moves in and out from the pulse tube room in room temperature T_{RT} from the He reservoir. When the pressure in the PT chamber is low, the gas is sucked inside the chamber with temperature T_{RT}. Later in the cycle it is pushed out from the chamber again when the pressure inside increase. As a consequence, its temperature will be higher then T_{RT}, meaning that the He flows out of the chamber hotter. In the heat

15
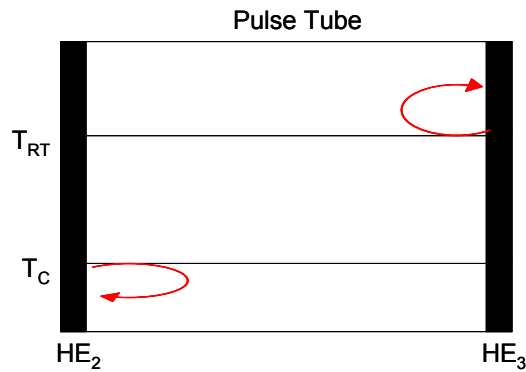
Figure 7: Gas elements enter in HE₂ with temperature T_c and leaves with lower temperature. In HE₃ the gas elements enter in room temperature and leave with higher temperature.

exchange *HE₃* the gas releases heat and cools back to T_{RT}. At the cooled end of the pulse tube chamber, an opposite effect occurs. Here the gas enters the chamber when the pressure is high with cold temperature T_c and when the pressure is lowered it leaves the chamber with temperature lower then T_c (see figure 6.a to 6.d cycle). In this way, the gas takes heat from *HE₂*, the cold finger of the system.

The Joule Thompson part of the system is expected to cool the system down to 1.5K. The basic idea behind the JT mechanism is thermodynamic as the PT and deals with expansion and contraction of Helium gas. The JT, called after Joule-Thompson effect describe the temperature change of gas or liquid when it is forced through a valve (in our case, needle valve) while isolated from the environment. At room temperature, all the gases except hydrogen, helium and neon cool upon expansion by the JT process. The definition of adiabatic expansion is $dq = 0$, (dq is the heat transfer) and it means that no heat goes in or out of the system. However, $dw \neq 0$ (*dw* is the work done by the system) meaning that as the gas expends it does some work on the surrounding. Since the gas is separated from any heat reservoir it can not drew heat from any source to convert it into work. The work must come from the internal energy of the gas, thus the internal energy decreases as required from the first low of the thermodynamics for ideal gasses. Since the internal energy of an ideal gas is dependent only on *T* it means that the temperature of the gas must decrease. It soon became apparent that the result of Joule expansion experiment was not valid for real gases. An additional and more accurate study was carried out by Joule and Thompson to investigate the properties of real gases under expansion. The
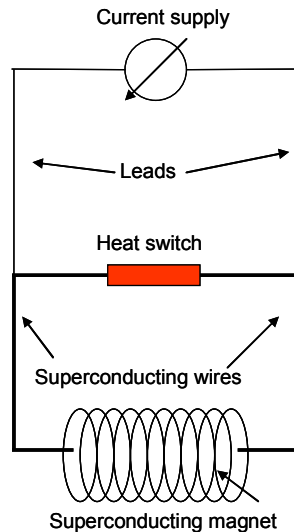
Figure 8: Drawing if the superconducting magnet system. The heat switch controls the persistence mode of the magnet.

experiment determined the JT effect coefficient (see appendix A). The coefficient gives information about the liquefaction of gases therefore provide the data on gas expansion while is cooled or heated. This coefficient has a decreasing dependence on temperature and it passes through zero at the JT inversion temperature T_I. By that, following JT expansion, it turns out that in order to liquefy a gas it must first be cooled below the JT inversion temperature. For He gas the JT inversion temperature is 40K. The gas is circulated in a closed-loop system by external pump. The pump forces the He gas through adjustable needle valve to obtain the JT effect. The gas in the circulation lines passes through cold trap to capture any moisture that could be present inside the system to prevent ice blockages in the JT. The cold trap is being sunk in liquid nitrogen and containing Zeolite minerals that are known in their moisture trap capabilities.

The third part of the system is the superconductor magnet. The magnet can reach 7 Tesla. Although the magnet operation temperature is 3.5 to 5K, the sample holder temperature can be adjusted from 1.5K to 300K without quenching the magnet.

For optical measurements, four windows are assembled on each side of the cryostat bottom. Both transport, adsorption and reflection measurements can be done with split magnet configuration as for having two coils that provide the horizontal magnetic field. Another advantage of superconductor magnet is the ability to operate in persistent mode. In this mode the superconducting circuit is close (by switching off the

magnet's heat switch) and perform superconducting continuous loop. In this stage the current from the DC power source can be taken out from the leads (see figure 8) to have a persistent mode that provides a noise free and permanent magnetic field.

The last section of the spectromag is the sample space, where the sample can be mounted onto a rod for the measurements. The sample holder can be stabilized over a wide range of temperatures from 1.5K to 300K. It is isolated from the system and only thermal linkers to the JT and PT helps to cool it down. The rod can be removed at any temperature without influencing the rest of the system parts temperature. Moreover, the sample space is filled with 1 atmosphere He gas at room temperature to enable good thermal contact.

2.2 Electrical measurements

In superconductors around the phase transitions the resistance falls down to zero and any "parasitic" resistances can influence the measurement. Therefore, it is essential to take into account the resistance of the contacts and the leads in the measurement setup. This is why any attempt to measure the superconductor with two probe configuration is problematic. To overcome this difficulty, a four probe configuration was used in all measurement. Two probes are connected as current suppliers and the two other connectors are used for voltage measurements. The voltmeter reads only the voltage that falls on the superconductor and hence the resistance of the sample.

The exact measurement configuration is presented in figure 9. In short, four conducting wires are attached to the film surface through two contacts that are used for voltage measurement and two for current.

The four wires were connected to the rod and to vacuum sealed connectors (described in the previews sub chapter). The current was supplied by Keithley 6221 DC and AC current source. The voltage was measured on the inner contacts by Keithley 2182A nano-voltmeter.
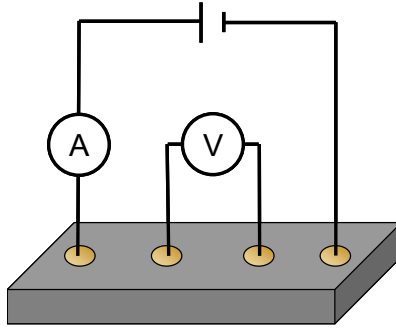
Figure 9: Four probe configuration scheme. Two of the wires are connected to DC current supply and two additional wires are connected to Voltmeter.

2.3 Sample method

2.3.1 Nb superconductor characterization and method

Niobium (Nb) is one of the three pure elements that exhibit type II superconductivity and has the highest *Tc* of the three, ~9.3*K* [33]. It is difficult to obtain a pure, single crystal Nb films due to its ability to append any materials in the process, especially gasses from the sample chamber[34].

There are few methods to prepare pure Nb film that preserve superconductivity properties. In my experiment, we used two kinds of methods to produce a single crystal, relative pure Nb type II superconductor. The first was by evaporation technique[33] and the second was by sputtering technique[35]. In this study, we were using both techniques and the Nb superconductor samples were realized in different thicknesses. Although there were differences in the thicknesses, only slight differences in the critical temperature and other properties of the samples were found. The differences can evolve from surface roughness, aggregation[35] and from diverse of impurities [33,34].

E-beam evaporated samples were grown on a sapphire substrate to reduce the Nb strain evaporation. The sapphire substrate appears as common substrate for Nb evaporation techniques.[35] In the evaporation process we were able to produce only few samples at one cycle. In addition, as the conditions were slightly different for each
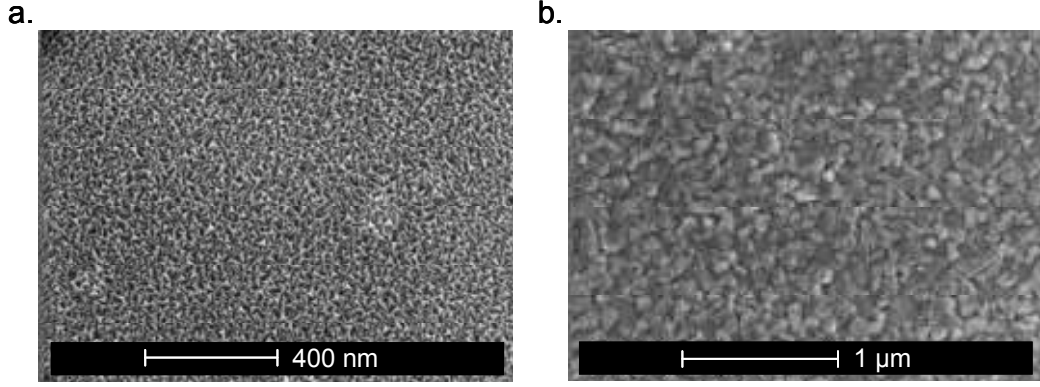
Figure 9: SEM pictures if Nb surface fabricate by e-beam evaporation (a.) and by sputtered (b.) techniques.

evaporation cycle, the properties of the samples changed from cycle to cycle making it hard to grow enough samples for a full set of measurement. Therefore, the sputtering technique (Nadav Katz Lab) was chosen as the preferred one, depositing 2" Nb wafer in each round of growth to have around 50 identical samples. In this stage the highest purity was achieved with Nb film grown on aluminum-deposited silicon substrate. SEM images of the Nb film surface for both the e-beam evaporation and sputtered techniques samples can be seen in figure 9.

The roughness of the Nb surface was measured by atomic force microscopy (AFM) to give around 2-3 nm, the same order of magnitude for both the evaporation and sputtered techniques (see figure 10).

It has well known that the T_C of Nb superconductor depends on the thickness of the sample [33,34]. This phenomenon was first explained by Cooper[36] as he related the effect to the surface electron-phonon interaction. These interactions reduces the coupling parameter between the electrons, λ (in Nb $\lambda = 45\,\text{nm}$). In the limit of films that are thinner then the superconductor's coherence length, ζ (in Nb ζ=38 nm), having a very thin surface layer (a), $a < \zeta$ Cooper predicted the Tc dependence on sample thickness should be written as

$$(2) \qquad T_{c0}(d_s) = T_{c0}(\infty) \exp\left(\frac{-2a}{\lambda d_s}\right)$$

Where $T_{c0}(d_s)$ is the transition temperature of a film with a thickness, d_s, and $T_{c0}(\infty)$ is the bulk transition temperature. The reason for that dependency originates from
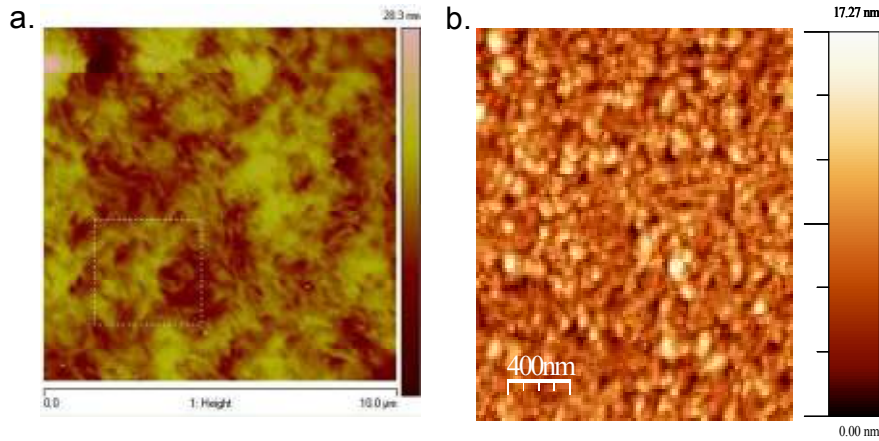
Figure 10: AFM measurement of the Nb surface fabricate by evaporation and sputtered techniques. The roughness of the evaporated sample is 3.5 nm (a.) and for the sputtered sample 3 nm (b.).

the *proximity effect* that exists between the bulk and the surface layer. Later works have revealed other explanations such as impurities and defects that can also be responsible to the T_C reduction in thin films. Another reason for the change in the critical temperature of thin films may be related to the native oxide layer on the surface of the Nb superconductor films. This layer which grows with time weakens the superconductivity thus responsible to the change in Tc.

The oxide layer of the Nb can contain more than 3 different types of layers. The most common layers are NbO, NbO_2 and Nb_2O_5.[37] The Nb_2O_5 layer exhibits dielectric properties while the NbO exhibits metallic like behavior. In order to improve the films uniformity, efforts were made to realize Nb superconductor films that contain only one type of oxide layer.[37] That was achieved by heating the sample in the evaporation process to 500 Celsius degrees for 24 hours to reduce the NbO, NbO_2 layers and produced only Nb_2O_5 layer.

2.3.2 Adsorption method

The hybrid structure of superconductor/ organic/ Au NPs was prepared by several sequenced adsorption steps as described below.

1. ***Cleaning the superconductor's surface***- The cleaning of the Nb surface was done by dipping the Nb samples in boiled solutions of acetone and isopropanol for 7 min and then placing in plasma Asher for 10 min. The the plasma asher cleaning adds 1 nm oxide layer to the already exist native oxide layer of the superconductors (as measured by ellipsometry).

2. ***Adsorbing the organic molecules***- The cleaned samples were inserted into a glove box under nitrogen atmosphere that was built especially for free-moisture impairment process. The substrates in the glove box were inserted into the organic molecule solutions. The solution concentration and solvent type were chosen with regard to the organic molecule type. For the diSilane and Hex diSilane molecules the concentration was 1mM in bicyclohexyl (BCH) for 2 min deposition. For MPS molecule the concentration was 10mM in BCH for 1.5 hours, and then they were dipped again for 1 more hour in the same organic solution. For OTS molecule the concentration was 1mM in Toluene for 2 min. The samples were then sonicated in Toluene for 1 min to remove any un-adsorbed organic residue and were dried under nitrogen flow.

3. ***Adsorbing of the Au nano particles*** - The samples with the assembled monolayers were inserted into 0.01% wt. stabilized tri-sodium citrate hydrated Au nano particles solution for 24 hour (product of Sigma).

The resulted samples were characterized by scanning electron microscopy (SEM), ellipsometry and by X-ray photoelectron spectroscopy (XPS) to ensure the adsorption of the Au NP's on top of the Nb superconductor and will be further discussed in the next chapter.

Chapter 3

3. Results and Discussion

3.1 Adsorption results and evidence for Au-Silane Bonds

In section 1.2.2, the use of self assembly as a tool to achieve an organic monolayer on top of the Nb superconductor and to attach gold nano particles was discussed. The chemical bonds between the Au NPs and the organic molecules allowing such attachments are well known with thiol head groups but are still controversial considering Silane-Au bonds. Our results show the existence of Si-Au bonds.

The first attempt to support the Au-Si bond was made by thoroughly washing the diSilane sample with acetone, ethanol and distilled water (DW) under sonication and hot toluene. Under this cleaning procedure the Au NPs were not removed as seen by SEM images presented in Figure 11. In contrast, Au NPs deposited on OTS (that does not exhibit Si-Au bond) were easily washed out. These results imply that a chemical bond between the silane to Au NP does exist.

To further characterize the chemical bond by X-ray photoelectron spectroscopy (XPS) were done. The Au doublet at 84.0 eV and 87.7 eV was identified only when the NP's were presented, compared to the bare Nb and Nb with only organic monolayer (figure 11.e).

The XPS measurements demonstrate peaks for Silicon and Carbon, (see figure 12) on top of the Nb surface after the adsorption of organic monolayer. This result proves that organic molecules are present on the substrate thanks to the adsorption.

To recognize the Au-Si chemical bond I adsorbed a monolayer of OTS molecule onto Au substrate. The XPS results show a reduced Si 2p *(I)* peak at 101.8 eV (Figure 13.a). Comparing these results to OTS molecules that were repeatedly dried by a nitrogen flow on top of the gold substrate, but were not adsorbed to it shows no peak at 101.8 eV, but instead at 102.6 eV (figure 12.b) indicating for oxidized Si-O bond. These results imply that the OTS monolayer exhibits Si-Au bond which is with agreement to previous studies.[38]
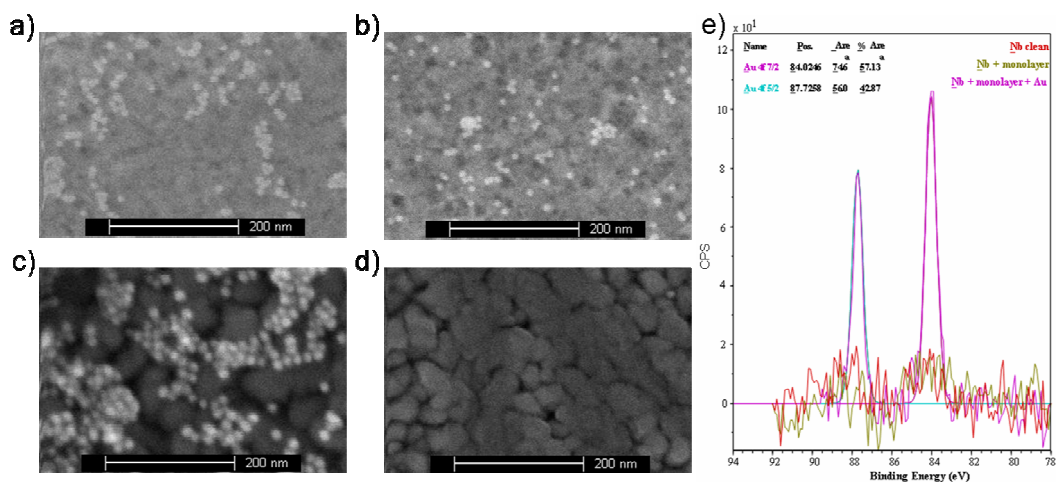
Figure 11. SEM images showing gold NPs (bright dots) adsorbed on top of an diSilane and OTS monolayer self-assembled on a gold film. after adsorption (a. and c. respectivily). After washing with acetone, ethanol under sonication and dipping in hot toluene (b. and d. recpectivly). XPS spectrum of the Au nano particles doublet at 84.0 eV and 87.7 eV. The red and green lines belong to bare Nb and Nb with an organic layer, respectively; the pink line belongs to the Nb with organic layer and Au particles.

Regarding the diSilane molecule it was impossible to recognize the Au-Si bond in the XPS due to screening of the Au-Si bond by Si-O-Si bonds. The diSilane molecule is very reactive and create multilayer when adsorbed on top of the substrate with Si-O-Si as bridges between the layers. The Si-O-Si bonds are found at 102.95 eV for Si 2p *(I)*. Another oxidized Si is seen at 103.54 eV for Si 2p *(II)* results from Si-OH groups indicating the layers are not fully oxidized to have all as Si-O-Si bonds as can be seen in figure 13.b.

	Ellispsometry	XPS	Molecule length
Hex diSilane	4.5 nm	----	1.1 nm
diSilane	3 nm	4.5nm	0.65 nm
MPS	0.5 nm	----	0.65 nm
OTS	3 nm	2.65nm	2.8 nm

Table 1. SAMs thickness as calculated by ellipsometer and XPS. The difference of the results from the molecular length can be caused by multilayer formation (diSilane, Hex diSilane) and monolayer tilt (MPS and OTS).
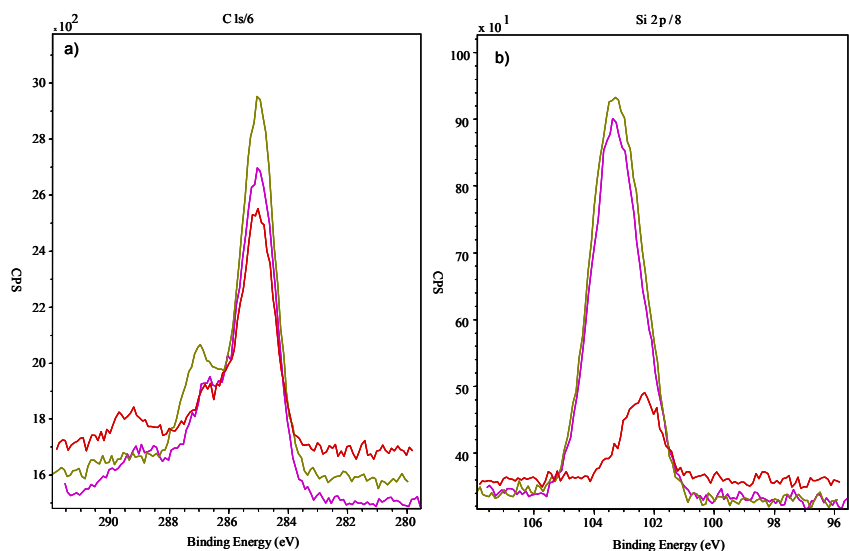
Figure 12: XPS measurement of Nb film clean (red), with monolayer (yellow) and after 10 Au NP's (pink) for Carbon at 285 eV correlate to C-C bond (a) and Silicon at 103.4 eV correlate with Si-O bond (b).

Another test to insure the existence of the self assembled monolayer (SAM) on top of our Nb substrate was done by ellipsometry and XPS thickness calculations. The results are summarized in Table 1. They confirm that the diSilane is not adsorbed as a monolayer but as a number of layers bound to each other by Si-O-Si bridges as found in the XPS.
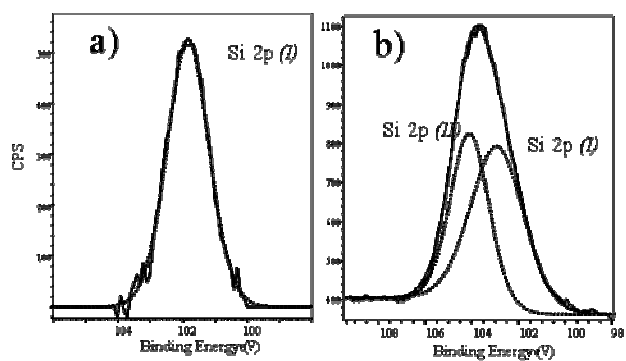
Figure 13. High resolution XPS spectra of Si 2p levels for a) OTS and b) diSilane samples.

In summary, the existence of organic monolayer and Au NP's adsorbed on the Nb surface was discussed. Moreover, I showed the presence of Au-Si bonds, therefore the Au NP's are chemically bond to the organic monolayer.

3.2 Peak effect as an indicator to coupling strength

One central issue in molecular electronics deals with charge transport across molecular elements. This aspect has turned into a flourishing research field at the interface between physics, biology, and chemistry.[39,40,41] However, despite significant progress many questions remained open.[42,43] Methods of conductivity measurements of single organic molecules essentially fall into two classes. Firstly, scanning tunneling microscope (STM) studies with an STM tip as a source electrode and a substrate layer as a drain.[39] Secondly, measuring molecular junction arrangement where a molecule is located in the gap between two conducting elements.[41,40]

In this section I present a hybrid system which combines gold nano particles (GNPs) connected to Nb superconductor via organic molecules that is sensitive to the GNPs-superconductor coupling and consequently to charge or energy transfer through the organic molecules. Hence, the superconductor acts as sensitive sensors that distinguish between the different ligand capping of the GNPs.

Our organic molecule capping ligands change the strength of the proximity effect between the GNPs and the type II superconductor. Any change in the superconductor properties due to the GNPs capping indicates that cooper pairs may tunnel through the organic layer from the Nb to the GNPs, or quasi particles may tunnel from the GNPs to the Nb substrate. Any of these mechanisms relates to the coupling efficiency of weak pinning centers created in the type II superconductor. The change in pinning efficiency can be measured by the enhancement of the superconductor critical current.[44] The superconductor's critical current variation in this case acts as a sensitive probe for the GNPs organic ligands capping coupling properties.

The sensitivity of the induced pinning is expected to increase in type-II superconductors around the peak effect.[45,46] Around this point the critical current density, measured as a function of the applied magnetic field H at a fixed temperature T, or as a function of T at fixed H, dramatically increase. In conventional low-T_c materials, this peak effect mainly occurs at magnetic fields H near the upper critical field $H_{c2}(T)$ and reflects a phase transition of the vortex lattice.[16] The vortex lattice is more fixable and therefore can fit better to the pinning landscape. In our measurements, we were able to

26

monitor the peak effect strength as a function of the organic molecule's layer length and study the consequent different coupling effects.

We have studied the coupling between the GNPs and Nb superconducting film, using well organized self-assembled organic monolayers. We used three types of organic linkers with different lengths (see figure 4) and therefore different coupling that were used in the study: diSilane, which forms a 3-nm-thick layer, MPS which forms a 0.5-nm-thick monolayer and Hex diSilane creating 4.5 nm thick layer. The strongest coupling is expected in the shortest MPS molecule while the weakest will occur in the Hex diSilsne. In the adsorption process a 50 nm Nb wafer was inserted into the different organic solutions and then into 10 nm Au NP's solution as discussed in section 2.3.2 of adsorption method. The electric measurements were performed using Oxford's beta-cryofree cooler with a four-probe point scheme as discussed in section 2.1 and 2.2 in chapter 2.

We expect that the peak effect will occur near the matching field, where the vortices creating by the magnetic filed will be of the same order of the NP's density. A calculation was made to evaluate the NP's density required. The total flux penetrating the superconductor is given by

$$\phi = \oint BdS = B \cdot S$$

Where B is the external magnetic field and S is a given closed area. In type II superconductors below H_{c2} the flux penetrates in the manner of vortices so the total flux is actually the sum of all the flux carried by the vortices.

$$\phi = \sum \phi_0 = n \cdot \phi_0$$

Where n is the total number of vortices and ϕ_0 is the vortex flux. Comparing the two equations and using the knowledge of a single vortex flux will predict the number of NP's required to pin the vortices.

$$n = \frac{S \cdot B}{\phi_0} = \frac{S \cdot B}{2.07 \cdot 10^{-7}}$$

The NPs density in all samples was approximately $2 \cdot 10^{10} \, dots/cm^2$. Hence, around 0.4 T the pinning density induced by the GNPs matches the density of the vortices penetrated to the superconductor (matching field). At this field, the enhancement of the critical current should be maximized. However, as the NPs adsorption is not uniform, we
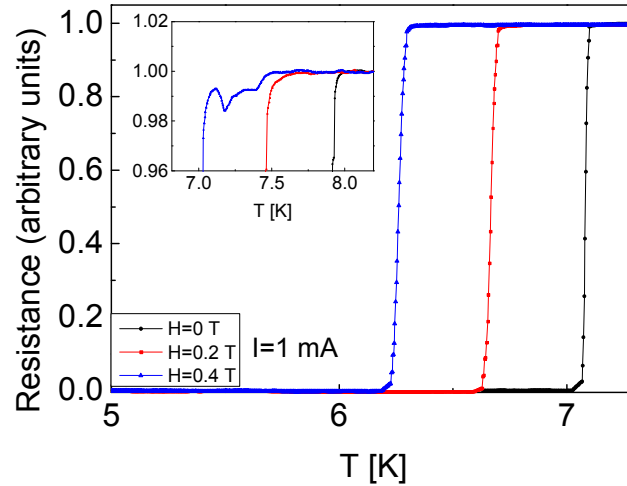
Figure 14: The resistance as a function of temperature for the bare Nb before the adsorption process in zero magnetic field (black), 0.2T magnetic field (red) and 0.4T (Blue). The inset shows the same data for the MPS molecule. A deep in the resistance or a peak in the critical current can be seen in 0.4T (blue).

expect that this maximum enhancement will be wide and change on different areas of the sample.

Figure 14 presents the first point that the peak effect appeared in a magnetic field of 0.4 T for the MPS molecule, compared to the bare Nb sample. The existence of peak effect after the adsorption for the MPS molecule implies that the adsorption process creates weak flux pinning in the superconductor that pins the vortices. Similar matching field, critical current enhancement (resistance deep) can be achieved also by ion implantations on the surface of superconductors.[10] For the bare Nb file, no peak effect could be recognized below 1.2T.

The peak effect existence was tested in the rest of the molecule systems to examine the molecules length dependence with the efficiency of the coupling. Figure 15 presents the resistivity as a function of the temperature at 0.4T for the three molecular systems. It is clear that at these conditions a peak in the critical current (a deep in the resistance) is measured only in the MPS with the shortest molecule and strongest coupling. The non uniformity in the distribution of the adsorbed GNPs on the Nb substrate creates fluctuations in the *deep* which depends on the contacts configuration.[47]
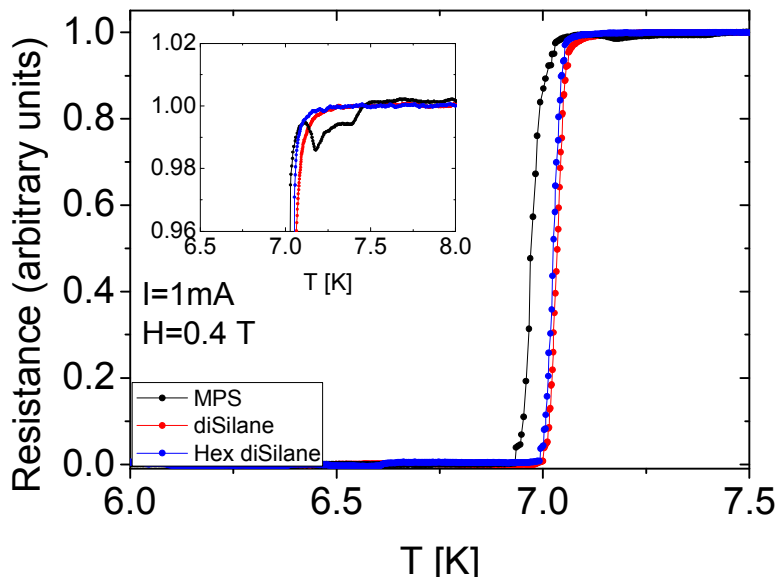
Figure 15: The resistance as a function of temperature for the three systems at 0.4T magnetic field applied: MPS (black), diSilane (red) and Hex diSilane (blue). The inset zooms in the peak effect area shows the peak effect for the MPS only.

We believe that this non uniformity is the origin of the peak effect complicated shape in our case. Nevertheless, the strongest phenomenon is seen when the magnetic matching field correlates with the GNPs density. These results suggest that the largest pinning contribution originates from the GNPs covered with the MPS ligands.

In this case the sample's initial pinning strength can be compared with the pinning induced by the charge transport through the organic molecules. Moreover, with the increasing of the magnetic field the peak effect becomes stronger.[48] Therefore, using the same system at higher magnetic fields will increase the sensitivity to weaker coupling. Changing the adsorption density will enhance the matching field and therefore the sensitivity. By controlling the density of the GNPs and the magnetic field, an estimation of the coupling probability can be achieved using the simple calculation above.

Figure 16 is showing the first field values at which the peak effect is seen in all three samples. Indeed, as we increase the magnetic field, the peak effect is starting to be recognizable at all three organic molecules. For the strongest coupling (MPS) the peak
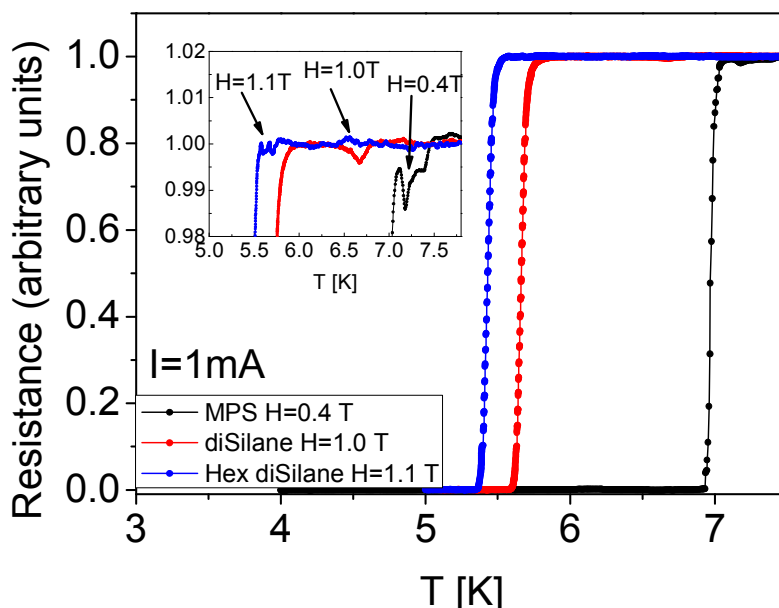
Figure 16: Normalized resistances of the Nb films as function of temperature for the three molecules used. The higher the magnetic field at which the peak effect is first observed the weaker the coupling of the molecule.

effect starts around 0.4T while the other molecules peak effect starts at higher fields above 1T. The weakest coupling is measured with the Hex diSilane system, where the thickness of the layer is the largest.

In summary, we have shown that the peak effect in superconductors can serve as an efficient sensor to distinguish between organic molecules that linked to the GNPs. The peak effect was sensitive enough to distinguish between three such linkers of different length. By tuning the superconducting film pinning strength, the GNPs adsorption density, and the magnetic field, the coupling efficiency of different molecules can be compared.

3.3 Increased superconducting transition temperature

The critical temperature, *Tc*, of superconductor is determined as the point which the resistance of the film falls to zero. This point is the phase transition between normal metal to superconductor state. The phase transition occurs as a collective effect of cooper pairing of electrons to a condensation state.

In this part of the work, we show that the superconducting critical temperature, T_C, of thin Nb films is significantly modified when gold nanoparticles (NPs) are chemically linked to the Nb film, with a consistent enhancement, when using 3 nm long diSilane linker molecules. The T_C increases by up to 10% for certain linker length and NPs size. No change was observed when the nanoparticles were physisorbed with non-linking molecules. We attribute these results to a pairing mechanism coupling electrons in the Nb and the NPs, mediated by the organic linkers.

We investigated the modifications of the superconductor transition temperature of 150 and 50-nm-thick Nb films due to adsorption of organic molecules and Au NPs. Two types of Nb films were used, one evaporated on sapphire and the other sputtered on Si wafers (as discussed in section 2.3.1). The films were coated with self-assembled monolayers of two types of organic linkers, to which the Au NPs were attached (see figure 4), diSilane and MPS. We also studied a sample covered by ~3 nm long non-linking (OTS) molecules, on which the Au NPs were only physisorbed and thus acted merely as a spacer layer. The thicknesses of the organic films were measured using an ellipsometer as well as by XPS (see Table 1 section 3.1). The Au NPs, either 10 or 5 nm in diameter, were attached to the organic molecules using the procedure described in section 2.3.2.

The electrical measurements were performed applying a four-probe configuration. The measured T_C values of the 150nm Nb films ranged from 7.8 K to 8.5 K and the magnetic field, normal to the sample surface, could be varied up to 1T. For the sputtered films, the superconducting transition width was ~0.05 K, implying that the Nb films were quite pure. All samples were cooled at zero magnetic fields, and the measurements were performed in the cooling direction using different currents. The presented results are the
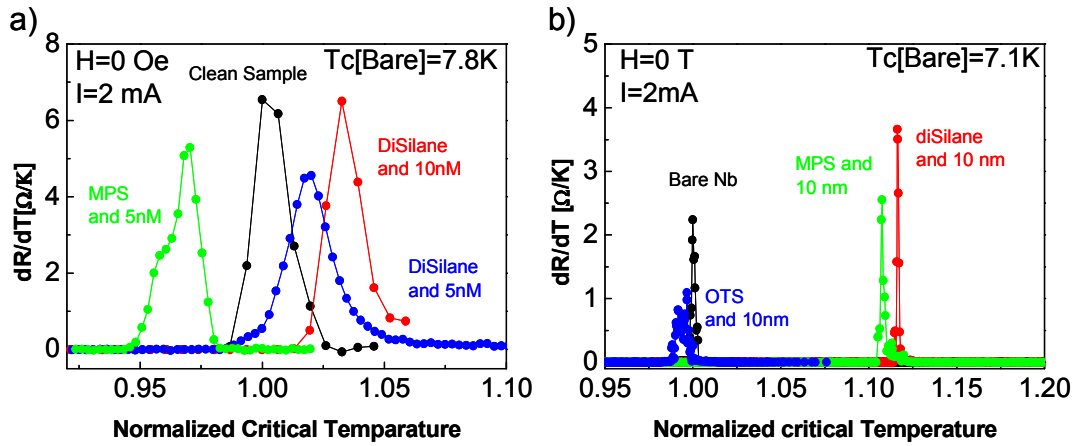
Figure 17: a) The differential resistance as a function of the normalized temperature measured at zero magnetic field. The temperature is normalized to T_C of the corresponding bare evaporated Nb film (Black). The blue and red curves show results obtained for samples with 5 and 10 nm Au NPs, respectively, linked to the Nb film via diSilane molecules. In green, data for 5 nm NPs linked by the MPS organic monolayer. (b) 50nm sputtered Nb film coated with 10-nm NPs linked by the diSilane and MPS organic layer showing about 10% increase in T_C. Very small changes in the critical temperature are observed when using non-linking OTS molecules. Note that the relative improvement of the 50 nm film is larger than that of the 150nm film.

ones with the highest current (highest signal to noise ratio) for which no heating effect was observed.

Figure 17.a presents the derivative of the resistance as a function of temperature, normalized to the T_C of the bare evaporated Nb film of thickness 150 nm. Data for the bare film (black curve) is shown as well as data obtained after the attachment of 5 and 10 nm diameter Au NPs with different organic linkers. The peak in each curve represents the normalized temperature of the given sample, as compared to the bare Nb film critical temperature which was 7.8K. When using the Nb film and short (MPS) organic linker, the binding of the Au NPs yields a reduction of the critical temperature. This reduction is more pronounced with the larger NPs (10 nm dia.) as compared with the small ones (5 nm dia.). These results are consistent with the expected PE and occurred also when the Au NPs were physisorbed directly on the surface of the Nb film. However, when longer linker molecules were used, a surprising increase in T_C was observed, by 3% for the 10-nm Au NPs and by 2% for the 5-nm Au NPs.

32
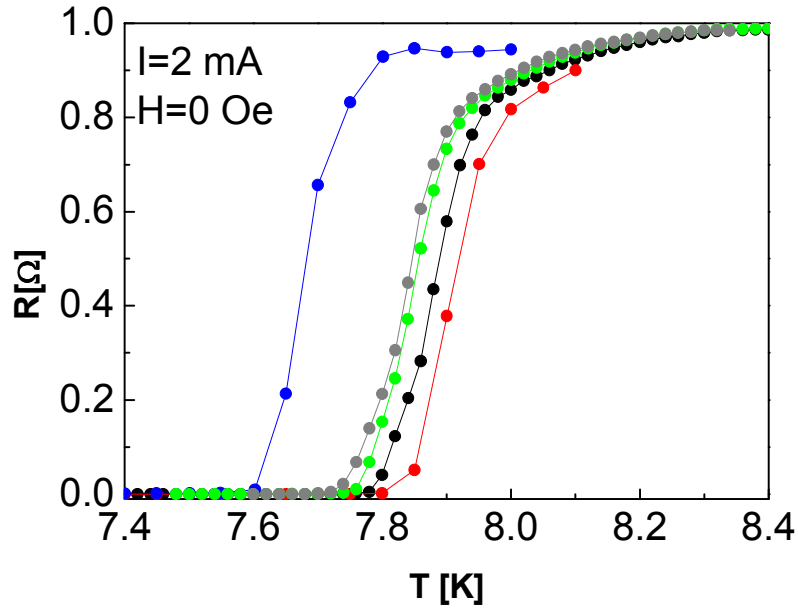
Figure 18: R(T) characteristics for 150nm Nb film: Blue- bare Nb substrate, Red- after diSilane adsorption and 10-nm Au NPs deposition. R(T) curves were then measured for the same sample, after partial removal of the organic layer and the Au NPs by plasma: Black- after 10 minutes plasma cleaning, Green- after 20 minutes plasma cleaning and Gray- after 60 minutes plasma cleaning. No effect of the plasma cleaning was seen on the bare Nb film.

Figure 17.b presents the measurements on the 50 nm thick sputtered Nb films coated with MPS and diSilane molecules to which 10 nm Au NPs were covalently attached. Here, an increase of about 10% in the critical temperature is measured for the MPS molecule (green curve), comparable to that measured for the diSilane molecule (red curve). For comparison, results are shown for the NPs physisorbed on the non-linking OTS layer (blue curve). A negligible effect on T_C is observed in this case, although the thickness of this layer is the same as that of diSilane. The widening of the transition fits the results of the phase transition, where only organic molecules are adsorbed.[22] This observation confirms that screening effects are not involved,[49] since here the OTS layer acts only as a spacer. We also find that the adsorbed monolayer by itself, with no NPs, does not affect the critical temperature consistent with Ref.[22]

The dependence of T_C on the density of the adsorbed Au NPs is demonstrated in Fig. 18, where the temperature dependent resistance, *R(T),* is presented for different NPs

densities. After deposition of 10 nm dia. Au NPs on the diSilane layer, T_C increased by 3% as compared with the bare Nb substrate. Removing the covalent bounded NPs is difficult, and only by applying plasma cleaning we were able to affect the organic layer. With the plasma, the organic monolayer was damaged and consequently the density of NPs was gradually reduced with each exposure to the plasma. Indeed, when the density of NPs was reduced, T_C decreased monotonically.

The above results suggest unique coupling that occurs between the electrons in the Nb film and in the NPs, mediated by the organic linkers. Such an effect is expected to manifest itself by modification of the electronic density of states (DOS) of the NPs and/or of the Nb film. The modification of the DOS will be discussed later in this chapter. The observed T_C enhancement effect is robust and does not depend (qualitatively) on the sample preparation procedure or the T_C of the bare Nb film (for the same film thickness). However, the magnitude of this effect does depend on the film thickness, the NP size, and the degree of coupling between the NPs and the Nb film.

In conclusion, we measured an enhancement of the critical temperature, which occurs when gold NPs are linked chemically to a superconducting Nb thin film. The observed effect depends on the NP's size, the length of the organic linkers, and the Nb film thickness. There are several mechanisms that may explain the observations, among them a pairing mechanism that involves coupling between electrons at the gold NPs and in the Nb film, mediated by the vibrations of the organic linker molecule as mentioned in section 1.1.4.

3.4 Increased superconducting critical current

In perfect superconductors current is flowing with no resistance, hence no power is dissipated. [44] Despite the seemingly practical importance of superconductors, their use is limited because of the need to work at very low temperature and the current density passing through them is relatively small. The reason to the limitations is caused by moving vortices that compel to move inside the superconductor due to Lorenz force. The critical current, Ic, is defined as the maximum current that can pass through the superconductor without forcing the vortices to move and to dissipated.

As expected, the change in critical temperature implied that pinning enhancement should result in change of the critical current. In what follows we show the critical current study in the hybrid layers.

It was previously demonstrated that a monolayer adsorbed on Nb film reduces the critical current.[22] The reason for such a behavior is the capturing of surface defected by the monolayer reducing the effective pinning force of the vortices.

Here we report that by adding the Au NP's an increase in the critical current is observed. Figure 19 present I/V measurement of a 50 nm Nb film before any treatment and after the adsorption of diSilane molecule only and diSilane molecule with 10 nm Au NP's. The measurement was performed below the critical temperature of the superconductor at 8 K without magnetic field. It shows that the critical current of the sample was suppressed with only molecules with agreement to Ref [22] and enhanced when it was attached to NP's.

More interesting to observe was the fact that every attempt to remove the organic linkers from the surface of the superconductor followed by reduction of the critical current as well as critical temperature (discussed above in figure 18). Figure 20 presents additional results for the cleaning process of Nb film coated by diSilane molecule and 10 Au NP's. The results show the critical current of the Nb before and after the adsorption and the three attempts to remove the organic substance with plasma cleaner. To calculate the critical current we chose a threshold value of 0.5mV and measured the Ic in wide temperature range.
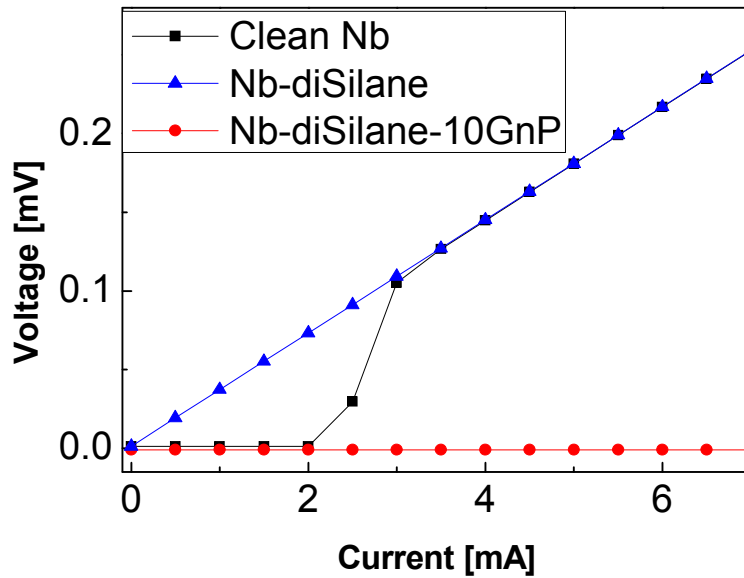
Figure 19: I/V charterstics of 50nm Nb superconductor film at 8K, just below the crtical tempratrure for superconductor transition. The black line presents data corrsespomnding to clean Nb film, where the crtical current (onset of voltage drop) is around 2mA. The blue line was measured on the same Nb film after diSilane adsorption, showing that the critical current is suppressed. The red line presents the situation after 10 nm gold NPs were deposited onto the diSilane, significantly enahancing the critical current to around 8 mA.

The results show an enhancement of the critical current after the adsorption of organic molecule and 10 nm Au NP's depositions. Moreover, when only molecules are adsorbed on top of the superconductor's surface we see a reduction in *Ic* indicating the major importance of the Au NP's for the effect.

The attempts to remove the organic substance from the superconductor have the same characteristic behavior as for the *Tc* reduction. The corresponding results are indicating that by removing the NP's density from the superconductor's surface, the *Ic* decreases.
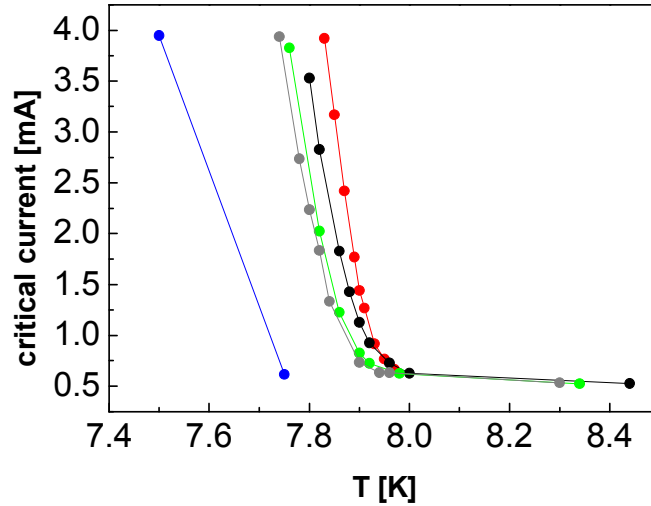
Figure 20: Critical current characteristics for Nb film as a function of temperature for: Blue- bare Nb substrate, Red- after diSilane adsorption and 10nm Gold NPs deposition. The data is presented, for the same sample, after partial removals of the organic layer and the gold NPs. Black- after 10 minutes in Plasma cleaner, Green- after 20 minutes in Plasma cleaner and Gray- after 60 minutes in the Plasma Cleaner. The data was obtained for current of 2 mA.. The data's are corresponding to the data in graph 17. The threshold voltage was fixed at 0.5 mV as Zero voltage.

To our understanding this behavior can occur when charge is transfer between the NP's to Nb film. In such case, the charge can induce a normal state in the superconductor and hence more pinning added to the surface. With this assumption, we can explain the enhancement of the critical current of the Nb film and the reduction when only molecules were attached. By assuming the "intrinsic" pinning density of the superconductor we can enhance the critical current by adsorbing a larger density of NP's. In the next sub-chapter I will discuss the matching field effect, when the density of vortices is of the same order as the NP's density.

3.5 Matching field effect

The increase in the critical current due to pinning mechanism was measured at different magnetic fields. In a type II superconductor, under an external magnetic field, penetration of Abrikosov vortex of magnetic flux is expected, where each vortex contains a flux quantum ϕ_0.[8] When the external magnetic field that perpendicular to the sample is increased, the density of the vortices increases proportionally and the Tc of the sample decreases. Simple calculation indicates that at a magnetic field of about 1 T, the density of the vortices should match the density of about $6 \cdot 10^{10}\ NP's/cm^2$. As the NPs are not ordered, below the matching field we should expect a decrease in the influence of the coupled NPs. Indeed, this effect is observed when comparing differences between the T_C at zero magnetic field, far from the matching field (Figure 21.a) and at 0.9T (Figure 21.b) closer to the matching field. In the later case the effect of the NPs, decreases significantly.

We relate the shoulder in the *R-T graph,* measured at 9000 G on the bare Nb film (figure 21.b, red curve) to vortex creep mechanism.[55] The disappearance of the shoulder after the attachment of the Au NPs indicates that the NPs provide efficient pinning centers, manifesting their electrical coupling to the Nb film.

To examine the possibility of matching field between the bare Nb samples to the adsorbed samples we extracted the data of the sample's critical temperature as a function of external magnetic field applied perpendicular to the sample surface. The data was fitted to the empiric equation

$$H_c(T) \approx H_c(0) \cdot \left[1 - \left(\frac{T}{T_c} \right)^2 \right]$$

Where $H_c(0)$ is the critical magnetic field at T=0 K and T_c is the critical temperature of the sample when $H = 0$ (figure 22).
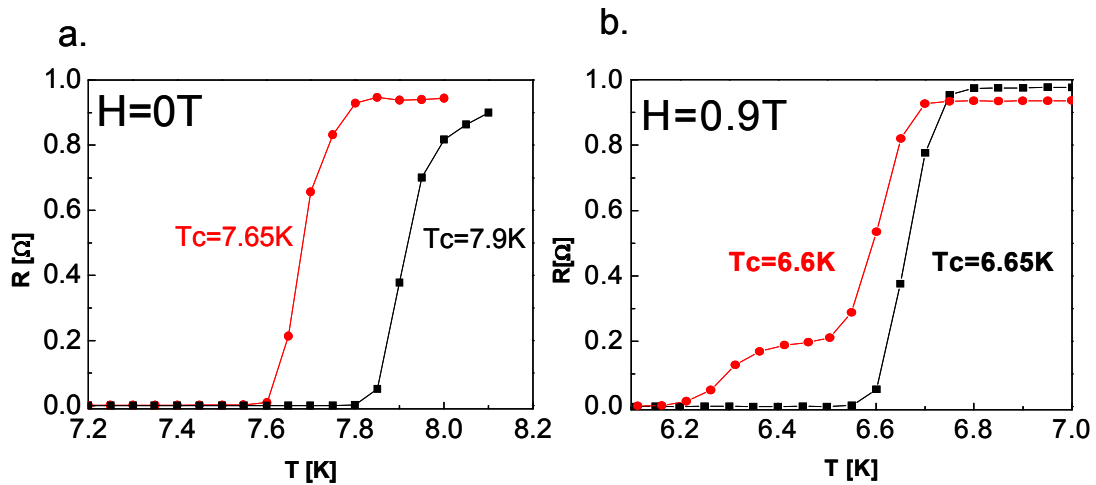
Figure 21: the resistance as a function of temperature for bare Nb (Red curve) and Nb after adsorption in diSilane molecules and 10 nm Au NP's deposition (Black curve) in the presence of perpendicular to the surface magnetic filed in: H=0 Tesla(a.) and H=0.9 Tesla (c.). The measurements were performed in 2mA.

Although the matching field depends on parameters like dots size, density and distribution, the intersection of the fitting curves may indicate that a matching field is exist and happens in H=1.86 T, a higher value that calculated with only dots density.
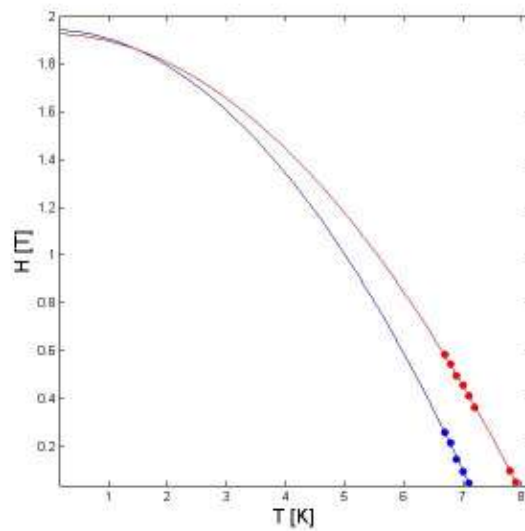
Figure 22: critical temperature as a function of external DC magnetic field perpendicular to the sample's surface for bare Nb film (Blue) and Nb adsorbed with diSilane molecule (red). The intersection of the fit curves may indicate of matching field.

In conclusion, the existence of a matching field indicates the strong coupling between the dots density to the vortices density. The trapping mechanism can be related to charge or energy transfer from the Au NP's to the Nb, which forms normal areas in the superconductor. Those areas acts like trapping sides that trap the vortices or vice versa Cooper diffusion to the Au NP's, that can induce superconductor behavior and trap the vortices. Therefore, higher dot density will increase the matching field.

3.6 Scanning tunneling microscopy and peak in the NP's DOS

The above results suggest unique coupling that exists between the electrons in the Nb film and in the NPs, mediated by the organic linkers. Such effect is expected to manifest itself by modification of the electronic density of states (DOS) of the NPs and/or of the Nb film. To study this effect, we performed electron tunneling spectroscopy measurements, using STM, on the various samples described above, at 4.2 K and at 15 K (below and above T_C). Zero bias anomalies, mostly peaks but occasionally also gaps in the DOS, were observed below T_C for samples in which the NPs caused a change in T_C. Figure 23 shows STM dI/dV versus V tunneling spectra acquired at 4.2 K on a 10 nm dia. GNPs. In this case the Au NPs (figure 23.a inset) were linked to a 50 nm thick Nb film through diSilane molecule. Such tunneling spectra, which are proportional to the local DOS, were numerically derived from I-V curves (figure 23.a). The figure presents a pronounced zero bias peak observed below T_C only, when measuring on Au NPs in samples that exhibit T_C enhancement. Above T_C, this peak vanished and the spectra became featureless (metallic-like). Such zero-bias peaks were observed for a wide range of bias or current set-points, being nearly reproducible for a given setting (figure 23.b), thus excluding the possibility that they are related to single electron charging effects.[56] However, the STM setting did affect the peak width, which ranged between 2 to 10 mV, and its height (figure 23.c). The tunneling spectra, measured over the organic layer far from Au NPs (in all samples), showed small gaps such as the one presented in the left inset to Fig. 23b. Fitting such a gapped conductance spectra to the Dynes DOS formula,[57] yielded superconducting gap values, Δ, in the range of 0.81-0.85 meV, somewhat smaller than the largest gaps reported for bare Nb surface, ~1.2 meV,[58] and relatively large broadening parameters, Γ ~0.32 meV, probably due to the presence of the organic molecules.

We occasionally found very shallow induced proximity gaps on NPs linked to the Nb via the short MPS molecules (figure 23.d), along with the conductance peaks observed on most of the other NPs. Such a gap is presented in the right inset of Fig. 23.b
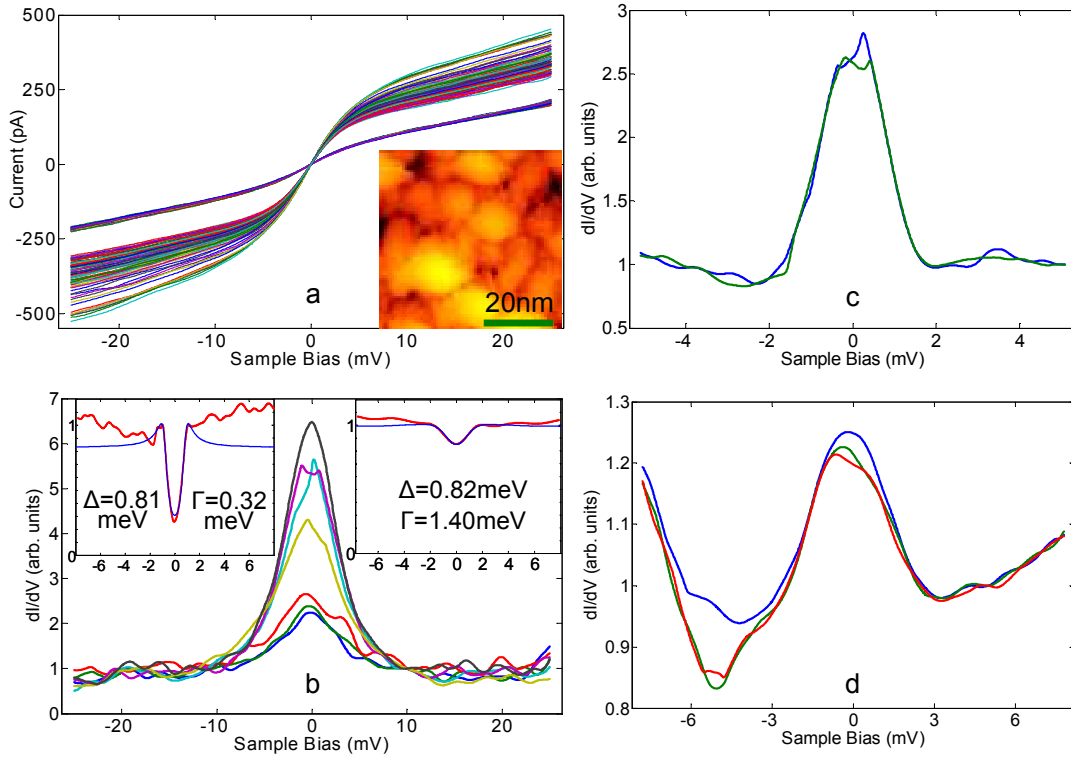
Figure 23: STM measurements showing the main spectroscopic features observed at 4.2K (below T_C). (a,b) – Tunneling spectroscopy measurements acquired on a single Au NP of 10nm diameter linked to diSilane grown on a 50nm Nb film, where the dI/dV-V tunneling spectra shown in (b) were derived from some of the I-V curves shown in (a). The spectra were acquired with a different bias voltage and current setting, in the range V = 5-7 mV and I = 40-110 pA, but all show a pronounced zero-bias peak, indicating that this peak is not due to single electron charging. The inset to (a) depicts a topographic image acquired at 4.2K on the same sample, focusing on a region dense with Au NPs. (c) – Tunneling spectra acquired on top of a single Au NP of 10nm diameter linked to a 50 nm Nb film via diSilane molecules. (d) – same as (c) but for the shorter MPS molecules. The measurements (a-d) were acquired on samples that showed an enhancement of T_C. The insets to (b) show dI/dV-V measurements (red) acquired on a Au NP (right) and the MPS covered Nb surface. The blue lines are fits to the Dynes function (see text), with the parameters indicated.

and could be fitted to $\Delta = 0.8$ meV and $\Gamma = 1.4$ meV. This may relate to our observation that the MPS molecules can lead to either enhancement or reduction in T_C. The latter behavior is typical to the conventional *proximity effect*. However, the induction of a proximity gap through the linker molecule, suggesting Andreev reflections through them, is still unexpected, in spite of the fact that they were observed in Anderson insulators.[59] It should also be pointed out that the absence of single electron charging effects, in this sample, suggests that the chemically linked NPs are well coupled electronically to the Nb film. It is important to emphasize that zero bias conductance peaks and gaps were

observed only for samples which showed a change (enhancement or reduction) in T_C. In samples where the NPs were physisorbed on the OTS molecules, a different behavior was observed, and the tunneling spectra frequently exhibited single electron charging effects.[56]

In conclusion, the STM measurement indicates that a coupling between the Au NP's to the organic molecules exist. When the molecules are short, the coupling is the strongest and the Au NPs show the standard proximity gap. When the dots are physisorbed, the coupling is very week and the Au NPs show the standard coulomb blockade charging spectrum. Only with intermediate coupling a new phenomenon is found where zero bias peak in the Au NPs density of states is observed. This peak in the DOS of the NP's is not yet fully understands.

Chapter 4

4. Proposed models

Several mechanisms were discussed in the literature that may contribute to the observed effect. Among them are enhancement of superconductivity by Anderson localization, induced by pair pinning in the vicinity of the NPs,[50] or suppressing the surface phonon effect that tend to reduce the T_C of the bare thin Nb films.[51] Another approach is to relate our results to a mechanism suggested by Leggett et al.[52,53] for high T_C superconductors,[52,60] in which Coulomb interaction between neighboring CuO_2 plains changes the Cooper pairing Hamiltonian and thus increases the inter-plain coupling. In our case, Coulomb interaction between the Nb film and in the gold NPs may influence the Cooper pairing.

The T_C increase may also be attributed to the coupling between the electron states on the Au NPs and electrons in the Nb, which introduces mixing of states without significant charge transfer. Such mixing may give rise to the zero bias anomalies observed in our tunneling spectra. This approach is related to the Ginsburg prediction,[54] which was proposed for geometry similar to ours.

Chapter 5

5. Summary

In the work presented here, I showed that by obtaining hybrid system of superconductor/ organic/ metal NPs, heterostructure I was able to change the properties of the superconductor and to monitor charge transfer through the molecules.

We experimentally measured an enhancement in the critical temperature and current of Nb superconductor, which occurs when gold NP's are linked chemically through organic molecules to the Nb thin film. When the NP's were only physoadsorbed on the organic molecules, an opposite results were achieved, implying that the chemical bond between them is of a major role in the enhancement of the superconductor's properties and for the peak in the NP's DOS.

The observed effects depended on the NPs' size, the length of the organic linkers, and the Nb film thickness. Tunneling spectra acquired on the linked NPs, below T_C, exhibited typically zero-bias peaks and occasionally, for the shorter linkers only, also induced proximity gaps, a known behavior in proximity effect field. Those results imply on optimization length of the molecule required to enhance the superconductor's properties.

There are several mechanisms that may explain the observations, among them a pairing mechanism that involves coupling between electrons at the gold NPs and on the Nb film, mediated by the vibrations of the organic linker molecule (Ginzburg prediction). However, the aforementioned mechanisms do not explicitly account for the peak in the density of states observed in the tunneling spectra. The experimental observations presented here provide new insight into the interaction between superconductivity and metallic nano particles. However, full understanding of the effect requires further theoretical and experimental exploration.

Finally, the sensitivity of superconductor to surface changes can serve as an indicator to charge or energy transfer to it through the organic layer.

Chapter 6

6. Future work

- **Improving the measurement system** - the system today can only perform DC transport measurements. The major drawback is the relative high current that it used to get the best signal to noise ratio. High current that pass through a thin superconductor film can cause a hitting effects that influence the measurement. To improve signal to noise ratio while lowering the currents a Lock-In Amplifier and AC current source can be used.

- **Optimization of the system parameters** – unfortunately, not all of the system parameters could be fully investigated at that time. The changing of the superconductor material, organic molecules type and length, and nano-particles type and diameters could influence dramatically on the effects described in this work. For example the change of the coupling strength with conjugated molecules or ferromagnetic nano particles are just two of many parameters that could investigated under this work.

- **High Tc superconductors** – the possibility of critical temperature enhancement in high Tc superconductors is intriguing. The complexity of the high Tc ceramic materials and different, two dimensional (layers) superconducting mechanism can be investigated with our hybrid system.

- **Magnetic induction measurements** – to get a new perspective of our results we want to perform a set of measurements with magnetic induction. These measurements can complete our transport and STM measurements and can tell us crucial information of the superconductor surface changing that took place before and after the adsorption.

- **Light influence** – excitation by light can affect the polarity and coupling strength of the molecule and can cause a Plasmon field in the Au NP's. Those effects are very intrusting to explore and can influence the enhancement of the effect we presented so far.

We have preliminary results showing the large influence of light on the superconductor film system using diSilane molecules and Au NP's deposition. Although, photon with energy larger then the superconductor's energy gap are suspected to break copper pairs and hence weaken the superconductor, it is not clear why the 526nm wavelength LED had less influence then the other wavelengths. We suspect that we see a plasmonic effect.

In figure 24 I present the resistance as a function of temperature of Nb film before and after the process. We can see that this sample showed enhancement of critical temperature. In addiction, the graph contains four measurements of the improved sample under LED illumination at different wavelengths. The optical output of the LED's was the same, which means that more photons are emitted from the longer (red, 660 nm LED) wavelength then the shorter wavelength (blue, 470 nm LED). More photons means more cooper pairs breaking and hence, weaker superconductor. From that point of view we could expect that the weaker properties will induced in the red LED and the stronger properties in the blue
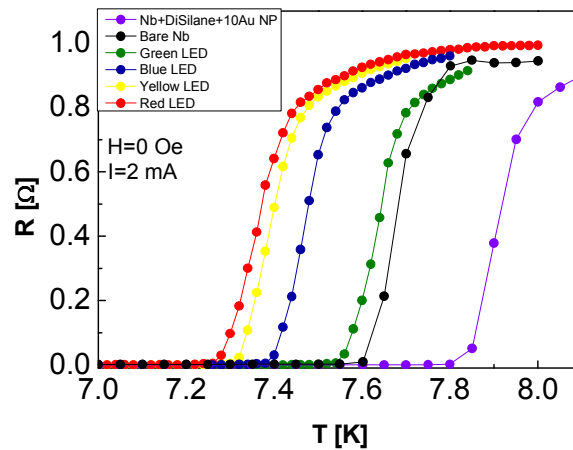
Figure 24: critical temperature results for: Nb adsorbed with diSilane molecules and 10 nm Au NP's (purple), Bare Nb film (black). The other results are LED emission in four different wavelengths: 526 nm (green), 470 nm (blue), 596 nm (yellow) and 660 nm (red).

LED. Surprisingly the very preliminary results show that under the green LED emission the superconductor gave the highest critical temperature. These results may be related to Plasmon field effect.

Appendix A: The Joule Thompson coefficient

As discussed in chapter 2 it became apparent that the results of the Joule expansion experiment were not valid for real gases. A more accurate experiment was carried out by Joule and J.J Thompson to further study the properties on real gases under expansion. For a real gas with a pressure P1, volume V_1 and temperature T_1, which is forced through valve coming out in the other side at pressure P_2, volume V_2 and temperature T_2 the change in temperature and pressure, are related.

In the following we assume that the system is isolated from the environment therefore $dq=0$. The work done in the process of passing through the valve can be divided to two; a) forcing the gas through the valve, and b) expanding the gas as it came out on the other side of the valve. The total work is

$$w = -P_1(0 - V_1) - P_2(V_2 - 0) = P_1V_1 - P_2V_2$$

Since $dq=0$, the change of the thermal energy of the gas is:

$$\Delta U = q + w = P_1V_1 - P_2V_2$$

The system's enthalpy is given by:

$$\Delta H = \Delta U + \Delta(PV) = P_1V_1 - P_2V_2 + P_2V_2 - P_1V_1 = 0$$

The JT experiment is a process at constant enthalpy. For small changes the ratio between the change in temperature and pressure could be approximate to a derivative.

$$\frac{\Delta T}{\Delta P} \approx \left(\frac{\Delta T}{\Delta P}\right)_H = \mu_{JT}$$

μ_{JT}, is the coefficient of Joule- Thompson effect. This coefficient is not zero for real gas. We see that if μ_{JT} is positive the dT is negative upon expansion so that the gas cools. On the other hand, if μ_{JT} is negative, then dT is positive so that the gas warms upon expansion.

In the original experiment Joule and Thompson could select a value for ΔP and measure the temperature difference ΔT. It turned out that the coefficient is a decreasing function of the temperature and it passes through zero at the Joule Thompson inversion temperature, T_I. In order to liquefy a gas by JT expansion the gas must first be cooled to below the JT inversion temperature.

Appendix B: Accepted paper- using the peak effect to pick the good organic couplers.

Using the peak effect to pick the good organic couplers

Eran Katzir, Shira Yochelis, and Yossi Paltiel[a]
Department of Applied Physics, Center for Nanoscience and Nanotechnology, Hebrew University, Givat Ram, Jerusalem 91904, Israel

Nanostructures are likely to become primary components of future electronic devices. Self assembled molecular electronics is a route to achieve this goal. One central issue in molecular electronics deals with charge transport across molecular elements. In this letter we present a hybrid system sensitive to the coupling and consequently to charge or energy transfer through organic molecules. Our system uses gold nanoparticles coupled through organic molecules layers to type II superconductor. We correlate the organic capping ligands of the gold nanoparticles with the vortices pinning efficiency. This sensitive phenomenon distinguishes between different organic molecules coupling efficiency. [doi:10.1063/1.3596434]

In recent years major improvements were achieved in fabrication and characterization techniques, down to the nanoscale resolution. This approach creates many opportunities and may open a way for developing quantum nanoengineered features. However, the practical realization of room temperature operating quantum devices faces a number of major challenges. Breakthroughs are required before an advance generation of quantum electronics can be achieved. One such approach is the use of self assembled organic molecules as the major building blocks of these devices.[1] Some molecular-based electronics include semiconducting devices with organic molecules as active components.[1-3] The self assembled organic molecules or group of molecules usually produce nanoscale network that present transport properties.[4-6] Presently, the field of molecular electronics is still at an early stage of phenomenological demonstrations.[1,7] Yet, it has already stimulated intense fundamental research.[8-10]

One of the central issues in molecular electronics deals with charge transport across molecular elements. This aspect has turned into a flourishing research field at the interface between physics, biology, and chemistry.[11-13] However, despite significant progress many questions remain open.[8,14] Methods of conductivity measurements of single organic molecules essentially fall into two classes. First, scanning tunneling microscope (STM) studies with an STM tip as a source electrode and a substrate layer as a drain.[11] Second, measuring molecular junction arrangement where a molecule is located in the gap between two conducting elements.[12,13] In both methods, test contacts between the molecule and the measurement system strongly influence the molecular state. An additional drawback is the fact that in most biological systems charge transfer occurs through ultrathin, two-dimensional (2D) supermolecular structures (SMSs) (Ref. 15) such as membranes and the extended 2D membranes cannot be probed by the above-mentioned "local" contact techniques. Recently, various experimental techniques have been adopted to study carrier transport properties of molecular membranes and self-assembled organic monolayers. Nevertheless, the charge transfer mechanism in 2D SMSs is far

from being well understood and it lacks the possibility of understanding complex structures and cooperative charge transfer in the system.[16,17]

We propose a hybrid approach which combines gold nanoparticles (GNPs) with organic molecules connected to a superconductor. The superconductor acts as a sensitive sensor that distinguish between the different ligands capping of the GNPs. Below the critical temperature, when GNPs are in proximity to the superconductor; proximity influence is expected to take place. The superconducting proximity effect is caused by diffusion of electron Cooper pairs into the normal material, and by the diffusion of electronic excitations into the superconductor. In general, proximity effect leads to depression of superconductivity in the superconductor, and it is well understood in classical BCS superconductors in the framework of de Gennes model.[18] Our organic molecule capping ligands change the strength of the proximity effect between the GNPs and the type II superconductor. Any change in the superconductor properties due to the GNPs capping indicates that cooper pairs may tunnel through the organic layer from the Nb to the GNPs, or quasiparticles may tunnel from the GNPs to the Nb substrate. Any of these mechanisms relates the coupling efficiency to weak pinning centers created in the type II superconductor. The change in pinning efficiency can be measured by the enhancement of the superconductor critical current.[19] The superconductor's critical current variation in this case acts as a sensitive probe for the GNPs organic ligands capping coupling properties.

The sensitivity of the induced pinning is expected to increase in type-II superconductors around the peak effect (or Fishtail effect).[20,21] Around this point the critical current density, measured as a function of the applied magnetic field H at a fixed temperature T, or as a function of T at fixed H, dramatically increase. In conventional low-T_c materials, this peak effect mainly occurs at magnetic fields H near the upper critical field $H_{c2}(T)$ and reflects a phase transition of the vortex lattice.[22] The vortex lattice is more fixable and therefore can fit better to the pinning landscape. In our measurements, we were able to monitor the peak effect strength as a function of the organic molecule layer length and study the consequent different coupling effects.

We have studied the coupling between the GNPs and Nb superconducting film, using well organized self-assembled

[a]Author to whom correspondence should be addressed. Electronic mail: paltiel@cc.huji.ac.il.
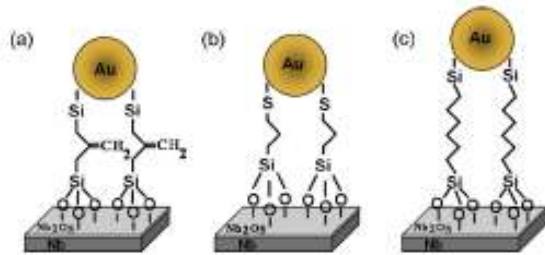
FIG. 1. (Color online) Schematic drawing of the experimental system. Cr/Au four-probe configuration contacts were evaporated on the Nb film. Self-assembled monolayers of three types of organic molecules were adsorbed on top of the sample. (a) 3-methylpropane bis-trichlorosilane, which forms a 3-nm-thick layer, (b) MPS, which forms a 0.5-nm-thick monolayer, and (c) 1,6-Bis(trichlorosilyl)hexane, which forms 4.5nm thick layer.

organic monolayers. Figure 1 presents three types of organic linkers with different lengths and therefore different coupling that were used in the study: (a) 3-methylpropane bis-trichlorosilane (DiSilane), which forms a 3-nm-thick layer, (b) mercapto propyl silane (MPS), which forms a 0.5-nm-thick monolayer and (c) 1,6-Bis(trichlorosilyl)hexane (Hex DiSilane) creating 4.5 nm thick layer. The strongest coupling is expected in the shortest MPS molecule while the weakest will occur in the Hex DiSilsne. Recently we have shown that in such system (Ref. 23) an improvement in the critical temperature can be measured with respect to the molecule length and type. In this letter, we study the peak effect under magnetic field changes, in clean Nb system with low GNPs adsorption density. In these conditions, the difference in critical temperatures is small and the main difference between the three organic layers linkers is the induced pinning strength in the superconductor.

The Nb 50 nm superconducting film was grown by sputtering on top of a 100 nm Al spacer to reduce lattice strain. In this way, high purity thin superconducting film was achieved (internal communication with Nadav Katz). Following the adsorption of the organic linker layer, the sample was inserted into a solution containing GNPs, 10 nm in diameter.[23] Figure 2 presents high resolutions scanning electron microscopy (HRSEM) of the GNPs on top of the Nb surface. The nanoparticles density in all samples was approximately 2×10^{10} dots/cm². Around 0.5 T the pinning density induced by the GNPs matches the density of the vortices penetrated to the superconductor (matching field).
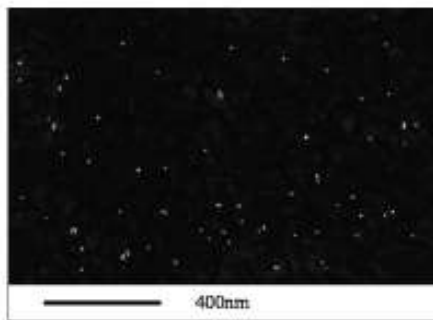
FIG. 2. HRSEM of the Nb surface coated with organic monolayer and 10 nm Au nanoparticles. The nanoparticles density is approximately 2×10^{10} dots/cm².
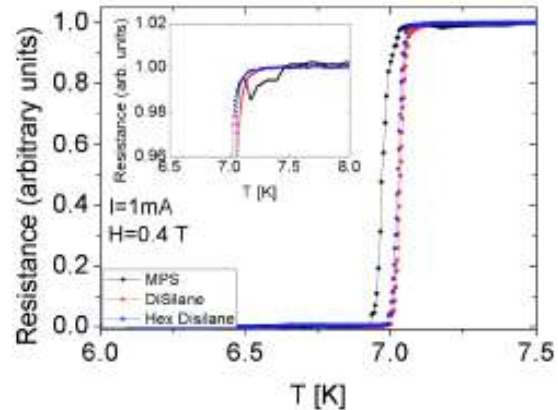
FIG. 3. (Color online) Normalized resistance of the Nb films as function of temperature. The molecules adsorbed on top of the film are DiSilane, Hex DiSilane and MPS. All measurements were performed at 0.4 T external, dc magnetic field. The inset shows a blow up of the peak effect area just below the Nb critical temperature. Only in the MPS system with the shorter length molecules a peak effect can be recognized.

At this field, the enhancement of the critical current should be maximized. However as the nanoparticles adsorption is not uniform, we expect that this maximum enhancement will be wide and change in different areas of the sample.

The electric measurements were performed using Oxford's beta-cryofree cooler with a four-probe point scheme. Figure 3 presents the resistivity as a function of the temperature at 0.4 T for the three systems. It is clear that at these conditions a peak in the critical current (a deep in the resistance) is measured only in the MPS with the shortest molecule and strongest coupling. The nonuniformity in the distribution of the adsorbed GNPs on the Nb substrate creates fluctuations in the deep which depends on the contacts configuration.[24] We believe that this nonuniformity is the origin of the peak effect complicated shape in our case. Nevertheless, the strongest phenomenon is seen when the magnetic matching field correlates with the GNPs density. This result suggests that the largest pinning contribution originates from the GNPs covered with the MPS ligands. In the MPS system at magnetic fields above 1 T additional phenomenon is seen. At these temperature and magnetic fields we identify an abnormality in the resistance. We relate this abnormality to surface superconductivity (H_{c3}).[25] As the temperature and magnetic field increase, communication between the superconducting layers is destroyed resulting in a crossover to 2D behavior.

In the relatively clean Nb system the peak effect is sensitive enough to distinguish between the three used molecules ligands that cover the GNPs. Further control of the system parameters can be achieved by changing the pinning strength, for example by ion implantation. In this case, the sample's initial pinning strength can be compared with the pinning induced by the charge transport through the organic molecules. Moreover, with the increasing of the magnetic field the peak effect becomes stronger.[26] Therefore, using the same system at higher magnetic fields will increase the sensitivity to weaker coupling. Changing the adsorption density will enhance the matching field and therefore the sensitivity. By controlling the density of the GNPs and the magnetic
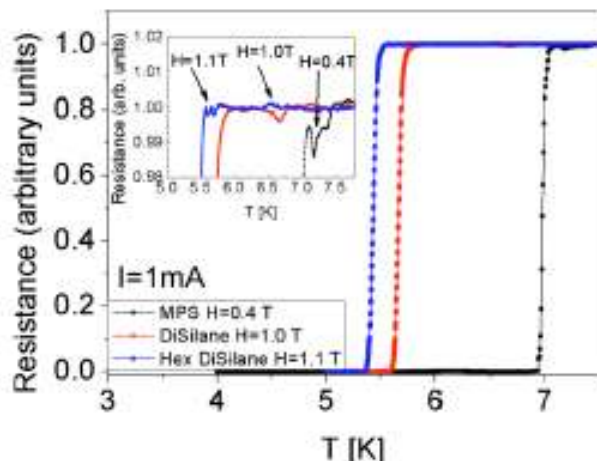
FIG. 4. (Color online) Normalized resistance of the Nb films as function of temperature for the three molecules used. The higher the magnetic field at which the peak effect is first observed the weaker the coupling of the molecule.

field an estimation of the coupling probability can be achieved using the simple de Gennes model.

Figure 4 is showing the first field values at which the peak effect is seen in all three samples. Indeed, as we increase the magnetic field the peak effect is starting to be recognizable at all three organic molecules. For the strongest coupling (MPS) the peak effect starts around 0.4 T while the other molecules peak effect starts at higher fields above 1 T. The weakest coupling is measured with the Bis(trichlorosilyl)hexane system where the thickness of the layer is the largest. For the clean Nb film, no peak effect was measured even at the highest field of 1.2 T. As a control experiment we also studied a sample covered by ~3 nm long nonlinking octadecyl trichlorosilane molecules, on which the Au NPs were only physisorbed and thus acted merely as a spacer layer. In this case the peak effect was measured at the same field where the peak effect appear in the clean Nb sample.

In summary, we have shown that the peak effect in superconductors can serve as an efficient sensor for differentiating between distinctive organic ligands that cover the GNPs. The peak effect was sensitive enough to distinguish between four such ligands of different length. By tuning the superconducting film pinning strength, the GNPs adsorption density, and the magnetic field, the coupling efficiency of different molecules can be compared.

[1]N. J. Tao, Nat. Nanotechnol. 1, 173 (2006).
[2]P. E. Burrows, S. R. Forrest, and M. E. Thompson, Curr. Opin. Solid State Mater. Sci. 2, 236 (1997).
[3]H. E. Katz and Z. Bao, J. Phys. Chem. B 104, 671 (2000).
[4]A. Nitzan and M. A. Ratner, Science 300, 1384 (2003).
[5]J. R. Heath and M. A. Ratner, Phys. Today 56,(5) 43 (2003).
[6]Processes in molecular wires, P. Hanggi, M. A. Ratner, and S. Yaliraki, editors, Special Issue Chem. Phys. 281, no. 2–3, 111-504 (2002).
[7]R. F. Service, Science 302, 556 (2003).
[8]C. P. Collier, E. W. Wong, M. Belohradsky, F. M. Raymo, J. F. Stoddart, P. J. Kuekes, R. S. Williams, and J. R. Heath, Science 285, 391 (1999).
[9]D. R. Stewart, D. A. A. Ohlberg, P. A. Beck, Y. Chen, R. S. Williams, J. O. Jeppesen, K. A. Nielsen, and J. F. Stoddart, Nano Lett. 4, 133 (2004).
[10]C. N. Lau, D. R. Stewart, R. S. Williams, and M. Bockrath, Nano Lett. 4, 569 (2004).
[11]L. A. Bumm, J. J. Arnold, M. T. Cygan, T. D. Dunbar, T. P. Burgin, L. Jones II, D. L. Allara, J. M. Tour, and P. S. Weiss, Science 271, 1705 (1996).
[12]M. A. Reed, C. Zhou, C. J. Muller, T. P. Burgin, and J. M. Tour, Science 278, 252 (1997).
[13]H. Park, J. Park, A. K. L. Lim, E. H. Anderson, A. P. Alivisatos, and P. L. McEuen, Nature (London) 407, 57 (2000).
[14]S. Lindsay, Faraday Discuss. 131, 403 (2006).
[15]A. P. H. J. Schenning, P. Jonkheijm, F. J. M. Hoeben, J. van Herrikhuyzen, S. C. J. Meskers, E. W. Meijer, L. M. Herz, C. Daniel, C. Silva, R. T. Phillips, R. H. Friend, D. Beljonne, A. Miura, S. De Feyter, M. Zdanowska, H. Uji-i, F. C. De Schryver, Z. Chen, F. Wurthner, M. Mas-Torrent, D. den Boer, M. Durkut, and P. Hadley, Synth. Met. 147, 43 (2004).
[16]H. B. Akkerman, P. W. M. Blom, D. M. de Leeuw, and B. de Boer, Nature (London) 441, 69 (2006).
[17]O. Seitz, A. Vilan, H. Cohen, J. Hwang, M. Haeming, A. Schoell, E. Umbach, A. Kahn, and D. Cahen, Adv. Funct. Mater. 18, 2102 (2008).
[18]P. G. de Gennes, Superconductivity of Metals and Alloys (Westview Press, Boulder, 1999).
[19]M. Tinkham, Introduction to Superconductivity (McGraw-Hill, New York, 1996).
[20]R. Wordenweber, P. H. Wes, and C. C. Tsuei, Phys. Rev. B 33, 3172 (1986); R. Wordenweber and P. H. Kes, Cryogenics 29, 321 (1989).
[21]S. Bhattacharya and M. J. Higgins, Phys. Rev. Lett. 70, 2617 (1993); M. J. Higgins and S. Bhattacharya, Physica C 257, 232 (1996).
[22]Y. Paltiel, E. Zeldov, Y. Myasoedov, M. L. Rappaport, G. Jung, S. Bhattacharya, M. J. Higgins, Z. L. Xiao, E. Y. Andrei, P. L. Gammel, and D. J. Bishop, Phys. Rev. Lett. 85, 3712 (2000).
[23]E. Katzir, S. Yochelis, G. Leitus, Y. Myasodeyov, B. Ya. Shapiro, R. Naaman, and Y. Paltiel (unpublished).
[24]C. Buzea and T. Yamashita, J. Optoelectron. Adv. Mater. 2, No. 5, 704 (2000).
[25]S. R. Park, S. M. Choi, D. C. Dender, J. W. Lynn, and X. S. Ling, Phys. Rev. Lett. 91, 167003 (2003).
[26]N. D. Daniilidis, I. K. Dimitrov, V. F. Mitrovic, C. Elbaum, and X. S. Ling, Phys. Rev. B 75, 174519 (2007).

Appendix C: Submitted paper's abstract

Increased superconducting transition temperature of a niobium thin-film proximity-coupled to gold nanoparticles using linking organic molecules

Eran Katzir,[1] Shira Yochelis,[1] Felix Zeides,[2] Nadav Katz,[2] Yoav Kalcheim,[2] Oded Millo,[2] Gregory Leitus,[3] Yuri Myasodeyov,[4] Boris Ya. Shapiro,[5] Ron Naaman,[6] and Yossi Paltiel[1]

[1]*Applied Physics Department and the Center for Nano-Science and Nano-Technology, the Hebrew University of Jerusalem, Jerusalem, 91904 Israel.*
[2] *Racah Institute of Physics the Hebrew University of Jerusalem, Jerusalem, 91904 Israel*
[3]*Chemical Support, The Weizmann Institute, Rehovot 76100, Israel*
[4] *Department of Physics, The Weizmann Institute of Science, Rehovot, 76100 Israel.*
[5] *Physics Department, Bar-Ilan University, Ramat-Gan, 52900 Israel*
[6] *Department of Chemical Physics, The Weizmann Institute of Science, Rehovot, 76100 Israel.*

Corresponding author: Yossi Paltiel- paltiel@cc.huji.ac.il

Abstract:

The superconducting critical temperature, T_C, of thin Nb films is significantly modified when gold nanoparticles (NPs) are chemically linked to the Nb film, with a consistent enhancement when using 3 nm long diSilane linker molecules. The T_C increases by up to 10% for certain linker length and NPs size. No change is observed when the nanoparticles are physisorbed with non-linking molecules. Electron tunneling spectra acquired on the linked NPs below T_C typically exhibit zero-bias peaks. We attribute these results to a pairing mechanism coupling electrons in the Nb and the NPs, mediated by the organic linkers.

Appendix D: Submitted paper's abstract- Formation of Au-Silane bonds

Formation of Au-Silane bonds

Shira Yochelis*, Eran Katzir, Yoav Kalcheim[#], Vitaly Gutkin[§], Oded Millo[#] and Yossi Paltiel

Department of Applied Physics, The Hebrew University of Jerusalem, Givaat Ram, Jerusalem, 91904, Israel.

[#] Physics Department, The Hebrew University of Jerusalem, Givaat Ram, Jerusalem, 91904, Israel

[§] The Unit for Nanocharacterization, The Center for Nanoscience and Nanotechnology, The Hebrew University of Jerusalem, Jerusalem, 91904, Israel.

CORRESPONDING AUTHOREMAIL: shirayo@cc.huji.ac.il

ABSTRACT: Many intriguing aspects of molecular electronics are attributed to organic-inorganic interactions, yet charge transfer through such junctions still requires fundamental study. Recently, there is a growing interest in anchoring groups, which considered dominating the charge transport. With this respect, we choose to investigate self assembly of di-Silane molecules sandwiched between gold surface and gold nanoparticles. These assemblies are found to exhibit not only covalent bonds between the anchoring Si groups and the gold surfaces, but also in plane cross links that increase the monolayer stability. Finally, using scanning tunneling spectroscopy we demonstrate that the di-Silane molecules provide strong electrical coupling between the Au nanoparticles and a metallic substrate.

Bibliography

1.   Onnes, H.K. The Superconductivity of Mercury. *Leiden Comm.* **120b, 122b, 124c**, (1911).
2.   Meissner, W. & Ochsenfeld, R. Ein neuer Effekt bei Eintritt der Supraleitf�higkeit. *Die Naturwissenschaften* **21**, 787-788 (1933).
3.   London, F. & London, H. The Electromagnetic Equations of the Supraconductor. *Proceedings of the Royal Society of London. Series A, Mathematical and Physical Sciences* **149**, 71-88 (1935).
4.   Bardeen, J., Cooper, L.N. & Schrieffer, J.R. Microscopic Theory of Superconductivity. *Phys. Rev.* **106**, 162 (1957).
5.   Bednorz, J.G. & Muller, K.A. Possible highT c superconductivity in the Ba-La-Cu-O system. *Zeitschrift fur Physik B Condensed Matter* **64**, 189-193 (1986).
6.   Cooper, L.N. Bound Electron Pairs in a Degenerate Fermi Gas. *Phys. Rev.* **104**, 1189 (1956).
7.   Ginzburg, V.L. & Landau, L..*Zh. Eksp Teor Fiz* **20**, (1950).
8.   Abrikosov, A.A. On the Magnetic Properties of Superconductors of the Second Group. *Soviet Physics JETP* **5**, 1174-1182 (1957).
9.   Civale, L. *et al.* Vortex confinement by columnar defects in YBa_{2}Cu_{3}O_{7} crystals: Enhanced pinning at high fields and temperatures. *Phys. Rev. Lett.* **67**, 648 (1991).
10.   Vélez, M. *et al.* Superconducting vortex pinning with artificial magnetic nanostructures. *Journal of Magnetism and Magnetic Materials* **320**, 2547-2562 (2008).
11.   Little, W.A. Possibility of Synthesizing an Organic Superconductor. *Phys. Rev.* **134**, A1416 (1964).
12.   Ginzburg, V.L. Nobel Lecture: On superconductivity and superfluidity (what I have and have not managed to do) as well as on the "physical minimum" at the beginning of the XXI century. *Rev. Mod. Phys.* **76**, 981 (2004).
13.   Larkin, A.I., Marchetti, M.C. & Vinokur, V.M. Peak Effect in Twinned Superconductors. *Phys. Rev. Lett.* **75**, 2992 (1995).
14.   Tang, C., Ling, X., Bhattacharya, S. & Chaikin, P.M. Peak effect in superconductors: melting of Larkin domains. *Europhysics Letters (EPL)* **35**, 597-602 (1996).
15.   Marchevsky, M., Higgins, M.J. & Bhattacharya, S. Two coexisting vortex phases in the peak effect regime in a superconductor. *Nature* **409**, 591-594 (2001).
16.   Paltiel, Y. *et al.* Instabilities and Disorder-Driven First-Order Transition of the Vortex Lattice. *Phys. Rev. Lett.* **85**, 3712-3715 (2000).
17.   Koopmann, J.A.G., Geshkenbein, V.B. & Blatter, G. Peak effect at the weak to strong pinning crossover. *Physica C: Superconductivity* **404**, 209-214 (2004).
18.   Kugel, K.I., Matsushita, T., Meilikhov, E.Z. & Rakhmanov, A.L. Fishtail or peak effect due to proximity in superconductor with normal inclusions. *Physica C: Superconductivity* **228**, 373-378 (1994).
19.   Sagiv, J. Organized monolayers by adsorption. 1. Formation and structure of oleophobic mixed monolayers on solid surfaces. *Journal of the American Chemical Society* **102**, 92-98 (1980).

20.   Sun, X., He, P., Liu, S., Ye, J. & Fang, Y. Immobilization of single-stranded deoxyribonucleic acid on gold electrode with self-assembled aminoethanethiol monolayer for DNA electrochemical sensor applications. *Talanta* **47**, 487-495 (1998).

21.   BAIN, C.D. & WHITESIDES, G.M. Molecular-Level Control over Surface Order in Self-Assembled Monolayer Films of Thiols on Gold. *Science* **240**, 62 -63 (1988).

22.   Shvarts, D. *et al.* Molecular induced field effect in superconducting Nb films. *Europhys. Lett.* **72**, 465-471 (2005).

23.   Wu, A.T. Investigation of oxide layer structure on niobium surface using a secondary ion mass spectrometry. *Physica C: Superconductivity* **441**, 79-82 (2006).

24.   Iler, R.K. *The Chemistry of Silica: Solubility, Polymerization, Colloid and Surface Properties and Biochemistry of Silica*. (Wiley-Interscience: 1979).

25.   Dadosh, T. *et al.* Measurement of the conductance of single conjugated molecules. *Nature* **436**, 677-680 (2005).

26.   Krygowski, T.M. & Stepień, B.T. Sigma- and Pi-Electron Delocalization: Focus on Substituent Effects. *Chemical Reviews* **105**, 3482-3512 (2005).

27.   Kulkarni, S.A., Mirji, S.A., Mandale, A.B., Gupta, R.P. & Vijayamohanan, K.P. Growth kinetics and thermodynamic stability of octadecyltrichlorosilane self-assembled monolayer on Si (100) substrate. *Materials Letters* **59**, 3890-3895 (2005).

28.   Mokrani, C., Fatisson, J., Guérente, L. & Labbé, P. Structural Characterization of (3-Mercaptopropyl)sulfonate Monolayer on Gold Surfaces. *Langmuir* **21**, 4400-4409 (2005).

29.   Fujimoto, Y., Heishi, M., Shimojima, A. & Kuroda, K. Layered assembly of alkoxy-substituted bis(trichlorosilanes) containing various organic bridges via hydrolysis of Si–Cl groups. *J. Mater. Chem.* **15**, 5151 (2005).

30.   Mansur, H.S. Quantum dots and nanocomposites. *WIREs Nanomed Nanobiotechnol* **2**, 113-129 (2010).

31.   Lindsay, S. *Introduction to Nanoscience*. (Oxford University Press, USA: 2009).

32.   Tews, M. Electronic structure and transport properties of quantum dots. *Ann. Phys.* **13**, 249-304 (2004).

33.   Wolf, S.A. Epitaxial growth of superconducting niobium thin films by ultrahigh vacuum evaporation. *J. Vac. Sci. Technol. A* **4**, 524 (1986).

34.   Wolf, S.A. Properties of superconducting rf sputtered ultrathin films of Nb. *J. Vac. Sci. Technol.* **13**, 145 (1976).

35.   Wildes, A.R., Mayer, J. & Theis-Bröhl, K. The growth and structure of epitaxial niobium on sapphire. *Thin Solid Films* **401**, 7-34 (2001).

36.   Cooper, L.N. Superconductivity in the Neighborhood of Metallic Contacts. *Phys. Rev. Lett.* **6**, 689 (1961).

37.   Proslier, T. *et al.* Improvement and protection of niobium surface superconductivity by atomic layer deposition and heat treatment. *Appl. Phys. Lett.* **93**, 192504 (2008).

38.   Gomez, S. *et al.* Gold nanoparticles from self-assembledgold(I) amine precursors. *Chem. Commun.* (2000).doi:10.1039/B005327I

39.   Bumm, L.A. *et al.* Are Single Molecular Wires Conducting? *Science* **271**, 1705 -1707 (1996).

40.   Park, H. *et al.* Nanomechanical oscillations in a single-C60 transistor. *Nature* **407**, 57-60 (2000).

41.   Reed, M.A., Zhou, C., Muller, C.J., Burgin, T.P. & Tour, J.M. Conductance of a Molecular Junction. *Science* **278**, 252 -254 (1997).

42.   Collier, C.P. *et al.* Electronically Configurable Molecular-Based Logic Gates. *Science* **285**, 391 -394 (1999).

43.   He, J. *et al.* Measuring single molecule conductance with break junctions. *Faraday Discuss.* **131**, (2005).

44.   Tinkham, M. *Introduction to Superconductivity: Second Edition*. (McGrew-Hill: New York, 1996).

45.   Wördenweber, R., Kes, P.H. & Tsuei, C.C. Peak and history effects in two-dimensional collective flux pinning. *Phys. Rev. B* **33**, 3172-3180 (1986).

46.   Bhattacharya, S. & Higgins, M.J. Dynamics of a disordered flux line lattice. *Phys. Rev. Lett.* **70**, 2617-2620 (1993).

47.   Buzea, C. & Yamashita, T. Structure anisotropy of high temperature superconductors: resistance peak effect. **2**, 704-712 (2000).

48.   Daniilidis, N.D., Dimitrov, I.K., Mitrović, V.F., Elbaum, C. & Ling, X.S. Magnetocaloric studies of the peak effect in Nb. *Phys. Rev. B* **75**, 174519 (2007).

49.   Bourgeois, O., Frydman, A. & Dynes, R.C. Inverse proximity effect in a strongly correlated electron system. *Phys. Rev. Lett* **88**, 186403 (2002).

50.   Burmistrov, I.S., Gornyi, I.V. & Mirlin, A.D. Enhancement of superconductivity by Anderson localization. *arXiv:1102.3323v1* (2011).at <http://arxiv.org/abs/1102.3323>

51.   Noffsinger, J. & Cohen, M.L. First-principles calculation of the electron-phonon coupling in ultrathin Pb superconductors: Suppression of the transition temperature by surface phonons. *Phys. Rev. B* **81**, 214519 (2010).

52.   Leggett, A.J. Cuprate Superconductivity: Dependence of Tc on the c-Axis Layering Structure. *Phys. Rev. Lett.* **83**, 392 (1999).

53.   Leggett, A.J. Some Thoughts About Two Dimensionality and Cuprate Superconductivity. *J Supercond* **19**, 187-192 (2006).

54.   Ginzburg, V.L. High-temperature superconductivity–dream or reality? *Sov. Phys. Usp.* **19**, 174-179 (1976).

55.   Coffey, M.W. & Clem, J.R. Unified theory of effects of vortex pinning and flux creep upon the rf surface impedance of type-II superconductors. *Phys. Rev. Lett.* **67**, 386 (1991).

56.   Hanna, A.E. & Tinkham, M. Variation of the Coulomb staircase in a two-junction system by fractional electron charge. *Phys. Rev. B* **44**, 5919 (1991).

57.   Narayanamurti, V., Garno, J.P. & Dynes, R.C. Direct Measurement of Quasiparticle-Lifetime Broadening in a Strong-Coupled Superconductor. *Physical Review Letters* **41**, 1509-1512 (1978).

58.   Richards, P.L. & Tinkham, M. Far-Infrared Energy Gap Measurements in Bulk Superconducting In, Sn, Hg, Ta, V, Pb, and Nb. *Phys. Rev.* **119**, 575 (1960).

59.   Frydman, A. & Ovadyahu, Z. Andreev reflections in Anderson insulators. *Europhys. Lett.* **33**, 217-222 (1996).

60.   Leggett, A.J. Some Thoughts About Two Dimensionality and Cuprate Superconductivity. *J Supercond* **19**, 187-192 (2006).

תקציר

ישנו קושי במדידה ובשליטה של מטען דרך מולקולה אורגנית. במחקר זה אנו מציגים שיטה חדשנית אשר רגישה למעבר אנרגיה מננו-חלקיקי זהב לעל-מוליך דרך שכבה אורגנית.

מקורה של הרגישות הרבה במדידה נובע *מתופעת הקרבה* המשנה את הזרם הקריטי של שכבת ניאוביום על-מוליך. השינוי בזרם מוסבר ע"י החזרת אנדרייב, כלומר מעבר מטענים מהננו-חלקיקים לניאוביום העל מוליך דרך השכבה האורגנית. החזרת אנדרייב גורמת באזורים מסוימים במוליך על למצב נורמאלי שמשמשים כאתרי מלכוד למערבולות הנוצרות בעל מוליך מסוג II. הוספת אתרי מלכוד מתורגמת בעליה בזרם הקריטי שאותה מדדנו.

הטמפרטורה הקריטית, T_C, בשכבות דקות של ניאוביום השתנו בעקבות צימוד של ננו-חלקיקים מזהב בעזרת מולקולות אורגניות. להפתעתנו הרבה גילינו שהטמפרטורה הקריטית מוגברת גם כאשר ספחנו עובי של 3nm~ *שכבה אורגנית*, כאשר עם מולקולה קצרה יותר צפינו בירידה בטמפרטורה הקריטית, כנראה עקב תופעת הקרבה ה"קלאסית". ההגברה שנצפתה ע"י המולקולה הארוכה או *תופעת הקרבה ה"הופכית"* הייתה עוצמתית אף יותר עבור אורך אופטימאלי של המולקולה, עד כדי % 10 ~ עבור עובי של 50nm ניאוביום.

האפקטים שחקרנו יכולים להיות מוסברים בעיקר ע"י מנגנון צימוד חדש המערב צימוד בין האלקטרונים בננו-חלקיק מזהב והעל-מוליך מסוג ניאוביום באמצעות הויברציות של המולקולות האורגניות.

האוניברסיטה העברית בירושלים

הפקולטה למתמטיקה ולמדעי הטבע

המחלקה לפיסיקה יישומית

הגברת תכונות על-מוליכות בשכבות דקות של ניאוביום, בצימוד לננו חלקיקי זהב בעזרת מולקולות אורגניות

ערן קציר

בהדרכת: ד"ר יוסי פלטיאל

עבודת גמר לתואר מוסמך במדעי הטבע

נובמבר 2011

תשע"ב